Stem Cell Reports
Article

ISSCR

OPEN ACCESS

Adhesion GPCR Latrophilin-2 Specifies Cardiac Lineage Commitment through CDK5, Src, and P38MAPK

Choon-Soo Lee,[1,2,5] Hyun-Jai Cho,[4,5] Jin-Woo Lee,[1,2] HyunJu Son,[1,2] Jinho Chai,[1,3] and Hyo-Soo Kim[1,2,3,*]

[1]Strategic Center of Cell & Bio Therapy, Seoul National University Hospital, Seoul 03080, Republic of Korea
[2]Molecular Medicine and Biopharmaceutical Sciences, Graduate School of Convergence Science and Technology, Seoul National University, Seoul, Republic of Korea
[3]Program in Stem Cell Biology, Seoul National University College of Medicine, Seoul, Republic of Korea
[4]Department of Internal Medicine, Seoul National University Hospital, Seoul, Republic of Korea
[5]Co-senior author
*Correspondence: hyosoo@snu.ac.kr or usahyosoo@gmail.com (H.-S.K.)
https://doi.org/10.1016/j.stemcr.2021.03.003

SUMMARY

Identifying lineage-specific markers is pivotal for understanding developmental processes and developing cell therapies. Here, we investigated the functioning of a cardiomyogenic cell-surface marker, latrophilin-2 (LPHN2), an adhesion G-protein-coupled receptor, in cardiac differentiation. LPHN2 was selectively expressed in cardiac progenitor cells (CPCs) and cardiomyocytes (CMCs) during mouse and human pluripotent stem cell (PSC) differentiation; cell sorting with an anti-LPHN2 antibody promoted the isolation of populations highly enriched in CPCs and CMCs. *Lphn2* knockdown or knockout PSCs did not express cardiac genes. We used the Phospho Explorer Antibody Array, which encompasses nearly all known signaling pathways, to assess molecular mechanisms underlying LPHN2-induced cardiac differentiation. LPHN2-dependent phosphorylation was the strongest for cyclin-dependent kinase 5 (CDK5) at Tyr15. We identified CDK5, Src, and P38MAPK as key downstream molecules of LPHN2 signaling. These findings provide a valuable strategy for isolating CPCs and CMCs from PSCs and insights into the still-unknown cardiac differentiation mechanisms.

INTRODUCTION

To take advantage of the beneficial properties of embryonic stem cells (ESCs) and induced pluripotent stem cells (iPSCs), the development of protocols for differentiating pluripotent stem cells (PSCs) into precursor and mature functional somatic cells is required. The demand for ESC- or iPSC-derived cardiomyocytes (CMCs) for use in cardiovascular disease research has increased in recent years (Fox et al., 2014; Oikonomopoulos et al., 2018). In addition, specific surface markers that enable monitoring of cell subtypes have been developed over the past several years to establish conditions that promote PSC differentiation into cardiac lineage cells (Oikonomopoulos et al., 2018).

A previous study showed that FLK-1 (also known as KDR or VEGFR-2) and PDGFR-α are co-expressed in the cardiac mesoderm (Kattman et al., 2011). These markers are expressed in both cardiac and vascular progenitor cells, but they appear transiently during development and require two-color flow cytometry for practical enrichment. Moreover, signal-regulatory protein α(SIRPα or CD172a) (Dubois et al., 2011) and podoplanin (PDPN) (Birket et al., 2015) have been used as surface markers for the selective enrichment and expansion of cardiac cell populations derived from human PSCs. Although several sets of cell-surface markers that distinguish cardiac progenitor cells (CPCs) from PSCs have been reported, the functional significance of these molecules remains elusive.

To develop a widely applicable strategy for the enrichment of PSC-derived cardiac cells, we conducted microarray screening to identify cell-surface markers specific to CPCs and focused on functional molecules, such as G-protein-coupled receptors (GPCRs) (Lee et al., 2019). GPCRs play an essential role in pathophysiology and represent attractive drug targets for the treatment of several diseases (Hilger et al., 2018). Recently, we discovered latrophilin-2 (LPHN2, Adgrl2) as a novel cell-surface marker for cardiomyogenic lineage cells during *in vitro* differentiation of mouse PSCs (Lee et al., 2019). LPHN2 is an adhesion GPCR characterized by large extracellular domains, and it has been reported to be ubiquitously expressed in multiple organ tissues of adult mice (Boucard et al., 2014). Another study showed that LPHN2 maintains synapse numbers through a postsynaptic mechanism in the mouse brain (Anderson et al., 2017). Although LPHN2 has been shown to play a role in the central nervous system, LPHN2 expression during cardiac differentiation and development and its clinical implication in heart disease are unclear.

Here, we demonstrate LPHN2 to be a functional marker for CPCs and CMCs during *in vitro* PSC differentiation. In addition, we investigate the underlying molecular mechanism of action of LPHN2 in cardiac differentiation. Our

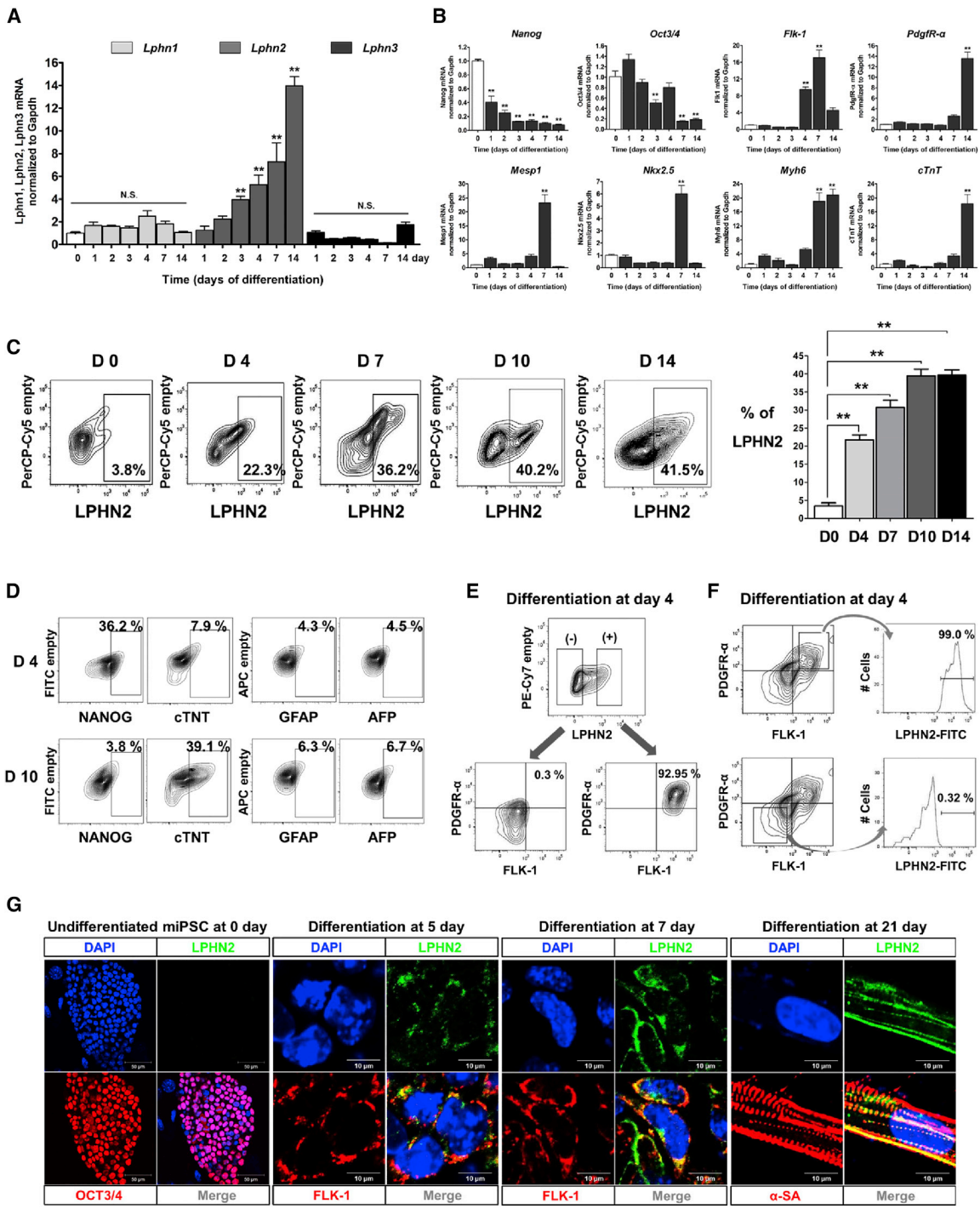

Figure 1. Expression Pattern of LPHN2 during Cardiac Differentiation

(A) Gene expression analysis of the latrophilin family in mouse induced pluripotent stem cells (iPSCs) during serial differentiation stages. Cultures of iPSCs under differentiation were harvested at the indicated days, and gene expression in cells was analyzed by qPCR. Values are shown relative to day 0. **p < 0.01, N.S., not significant, one-way ANOVA and *post hoc* Bonferroni test, $n = 3$ independent replicates.

(B) mRNA expression levels of *Nanog*, *Oct3/4*, *Flk-1*, *PdgfR-α*, *Mesp1*, *Nkx2.5*, *Myh6*, and *cTnT* in mouse iPSC-derived cells at successive stages during cardiac differentiation. **p < 0.01, one-way ANOVA and *post hoc* Bonferroni test, $n = 3$ independent replicates.

(legend continued on next page)

findings provide a vital strategy for achieving cardiomyogenic lineage cell differentiation.

RESULTS

LPHN2 Is Expressed in CPCs and CMCs during Mouse PSC Differentiation

To optimize the conditions for cardiac lineage cell differentiation, we compared the spontaneous and directed differentiation of mouse PSCs. Moreover, we established a protocol for directed PSC differentiation into CMCs after exposing cells to various combinations of cytokines for different periods, based on the biology of embryonic development (Greber et al., 2010; Hudson et al., 2012; Kattman et al., 2011; Laflamme et al., 2007; Yang et al., 2008; Yu et al., 2011). For the directed differentiation of mouse iPSCs into the cardiac lineage cells, embryoid bodies (EBs) were generated in an AggreWell plate after culturing for a day in EB medium in the presence of bone morphogenetic protein 4 (BMP-4), with the subsequent addition of activin A and basic fibroblast growth factor (FGF2) for 3 additional days (Figure S1A). On day 4, EBs were transferred to the cardiac differentiation medium containing epithelial growth factor, FGF2, cardiotrophin-1, and vascular endothelial growth factor (Lee et al., 2019). On day 14, we observed a 4.5-fold increase in the number of beating foci in cells undergoing optimized differentiation compared with that in cells undergoing spontaneous differentiation (Figure S1B). Immunofluorescence (IF) analysis of beating cells revealed a strong expression of α-sarcomeric actinin (α-SA) (Figure S1C).

We investigated the expression patterns of all three LPHN-family genes during differentiation. *Lphn2* expression gradually increased during cardiac differentiation and plateaued 14 days after induction of differentiation, whereas the expression levels of *latrophilin-1* (*Lphn1*, *Adgrl1*) and *latrophilin-3* (*Lphn3*, *Adgrl3*) remained unaltered (Figure 1A). Following induction of differentiation, the pluripotency genes *Nanog* and *Oct3/4* (*Pou5f1*) (Cho et al., 2010) were found to be downregulated, whereas the mesoderm and CPC markers (*Flk-1*, *Mesp1*, and *Nkx2.5*) were expressed transiently 7 days postinduction (Figure 1B). Similarly, the CMC markers *Myh6* and *cTnT* (Ieda et al., 2010) were highly expressed 14 days postinduction.

Flow cytometric analysis revealed LPHN2 expression on the surface of 41.5% of cells after 14 days of optimized cardiac differentiation (Figure 1C). Moreover, the expression of the pluripotency-related marker (NANOG) decreased during differentiation, and that of the cardiac lineage marker (cTNT) gradually increased (Figure 1D). The expression of the other lineage markers (glial fibrillary acidic protein and α-fetoprotein) did not change (Figure 1D).

To determine whether LPHN2 expression correlates with the expression of the CPC markers, we divided the cells into LPHN2-negative ($LPHN2^-$) and LPHN2-positive ($LPHN2^+$) subpopulations 4 days post differentiation. The $LPHN2^+$ population overlapped with the FLK-1^+PDGFR-α^+ (F^+P^+) population by 92.95%, validating LPHN2 as a CPC marker (Figure 1E). In addition, 99% of the F^+P^+ subpopulation expressed LPHN2, whereas only 0.32% of the FLK-1^-PDGFR-α^- (F^-P^-) subpopulation expressed LPHN2 (Figure 1F). Furthermore, immunostaining analysis revealed an absence of LPHN2 in undifferentiated cells; its expression gradually increased following induction of differentiation (Figure 1G). Moreover, LPHN2 co-localized with FLK-1 on day 7 of differentiation and α-SA on day 21 (Figure 1G).

To examine the expression of LPHN2 during differentiation of mouse PSCs into non-CMC cell types, we induced endothelial cell (EC) differentiation, as described previously (Joo et al., 2012). When FLK-1^+ mesodermal precursor cells were purified on day 4, *Cd31* expression was found to increase gradually in the EC differentiation medium (Figure S1D). IF staining showed that the $CD31^+$ EC colonies on day 21 did not express LPHN2 (Figure S1E), suggesting that LPHN2 was detected only in PSC-derived CPCs and CMCs from the mesoderm lineage.

To explore the broad-spectrum utility of LPHN2 as a cell-surface marker, we validated our findings by examining

(C) Flow cytometric analysis of LPHN2 expression during cardiac differentiation. (Left) LPHN2 expression in mouse iPSC-derived cardiac cells at various time points. (Right) Quantification of the plots shown on the left. $^{**}p < 0.01$, one-way ANOVA and *post hoc* Bonferroni test, $n = 4$ independent replicates.

(D) Flow cytometric analysis of cells on consecutive days after cardiac differentiation. NANOG was used as a pluripotency marker, cTNT as a CMC marker, glial fibrillary acidic protein (GFAP) as an ectoderm marker, and α-fetoprotein (AFP) as an endoderm marker.

(E and F) Representative fluorescence-activated cell sorting (FACS) plots showing the correlation between LPHN2 and co-expression of FLK-1 and PDGFR-α. FACS analysis for LPHN2 expression in differentiated cells at day 4 is shown. (E) The $LPHN2^+$ and $LPHN2^-$ cell populations were analyzed using anti-FLK-1 and anti-PDGFR-α antibodies. (F) The FLK-1^+/PDGFR-α^+ and FLK-1^-/PDGFR-α^- cell populations were divided, and LPHN2 expression was analyzed.

(G) Immunostaining for LPHN2 and OCT3/4, FLK-1, or α-SA in monolayer cultures in the early (day 7) and late (day 21) stages of cardiac differentiation. Blue, nuclear counterstaining with 4,6-diamidino-2-phenylindole (DAPI). PSC, pluripotent stem cell.

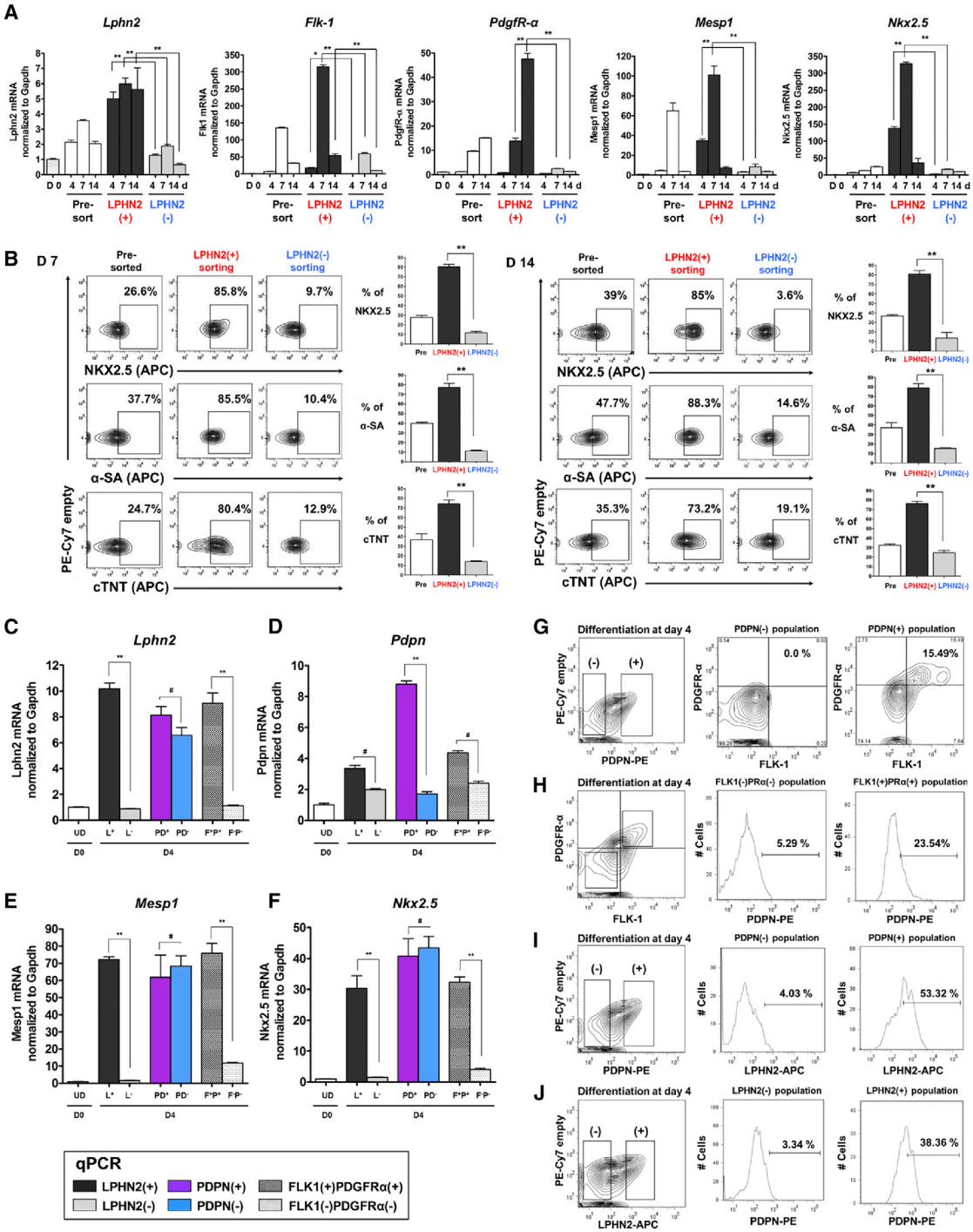

Figure 2. Enrichment of iPSC-Derived Cardiac Progenitor Cells and Cardiomyocytes by Cell Sorting Based on LPHN2 Expression

(A) qPCR analysis of cardiac lineage cell markers in pre-sorting and sorted (LPHN2$^+$ and LPHN2$^-$) cells at various stages of cardiac differentiation of iPSCs. Values are shown relative to day 0. *p < 0.05, **p < 0.01, one-way ANOVA and *post hoc* Bonferroni test; *n* = 3 independent replicates.

(B) Pre-sorting and sorted (LPHN2$^+$ and LPHN2$^-$) fractions at each time point were analyzed for NKX2.5, α-SA, and cTNT expression by intracellular flow cytometry. Quantification of the plots is shown on the right. **p < 0.01, one-way ANOVA and *post hoc* Bonferroni test; *n* = 3 independent replicates.

(legend continued on next page)

other mouse ESC (mESC) lines. mESC-derived CPCs and CMCs exhibited *Lphn2* gene and LPHN2 protein expression levels similar to those noted for iPSC-derived CPCs and CMCs (Figures S2A–S2D).

Enrichment of Cardiac Lineage Cells by LPHN2

To determine whether LPHN2 can be used as a marker to select populations enriched in the cardiac lineage cells, $LPHN2^+$ and $LPHN2^-$ fractions were isolated from mouse iPSC-derived cell populations after 4, 7, and 14 days of differentiation by cell sorting. The purities of the $LPHN2^+$ and $LPHN2^-$ sorted populations are shown in Figure S3. Gene expression analyses revealed higher expression of *Lphn2*, *Flk-1*, *PdgfR-α*, *Mesp1*, and *Nkx2.5* in $LPHN2^+$ cells than in $LPHN2^-$ cells (Figure 2A). After cell sorting on days 7 and 14, the $LPHN2^+$ fractions at both stages were dominantly enriched for NKX2.5, α-SA, and cTNT expression, representing CPCs and CMCs, compared with the $LPHN2^-$ fractions (Figure 2B). In addition, fluorescence-activated cell sorting (FACS)-based separation of various cell lines reproduced the significant enrichment of mESC-derived CMCs (Figure S4).

To investigate the feasibility of using LPHN2 as a cardiac-specific cell-surface marker, we assessed the advantages of using $LPHN2^+$ CPCs over cells expressing other known markers (Birket et al., 2015; Dubois et al., 2011; Kattman et al., 2011). Interestingly, quantitative real-time polymerase chain reaction (qPCR) analysis revealed that F^+P^+ cells expressed higher levels of *Lphn2* than F^-P^- cells, similar to $LPHN2^+$ cells (Figure 2C). Conversely, the difference in *Lphn2* expression between $PDPN^+$ and $PDPN^-$ populations was not significant. Moreover, *Pdpn* expression was not significantly higher in $LPHN2^+$ and F^+P^+ cells than in $LPHN2^-$ and F^-P^- cells, respectively (Figure 2D). The expression of *Mesp1* and *Nkx2.5*, which encode CPC markers, was higher in $LPHN2^+$ and F^+P^+ cells than in $LPHN2^-$ and F^-P^- cells, respectively (Figures 2E and 2F). However, the expression of CPC markers in the $PDPN^+$ cells was not higher than that in the $PDPN^-$ cells. Moreover, flow cytometric analysis demonstrated higher expression of F^+P^+ in $PDPN^+$ cells than in $PDPN^-$ cells; however, the expression was lower than that in the $LPHN2^+$ cells (Figure 2G). Conversely, F^+P^+ cells expressed a marginally higher level of PDPN than F^-P^- cells, suggesting that PDPN is not a functional receptor for mouse CPC differentiation (Figure 2H). The correlation between PDPN and LPHN2 was examined, and 53.32% of the $PDPN^+$ population was found to express LPHN2 (Figure 2I). In addition, 38.36% of the $LPHN2^+$ population expressed PDPN, indicating a low correlation between the LPHN2 and the PDPN markers (Figure 2J).

Taken together, these cell sorting analyses demonstrated that LPHN2 expression distinguished cardiac lineage cells during differentiation of mouse iPSCs and ESCs, and cell sorting with the anti-LPHN2 antibody allowed isolation of populations highly enriched in CPCs and CMCs.

Functional Significance of LPHN2 in Cardiac Differentiation

To examine the functional significance of LPHN2 *in vitro*, we used a short-hairpin RNA (shRNA) against *Lphn2* mRNA to knock down (KD) *Lphn2* expression in mouse iPSCs, achieving 70% reduction in *Lphn2* expression (Figures 3A and 3B). No differences were observed between control-iPSCs and *Lphn2*-KD cells in the expression of pluripotency-related genes (*Nanog* and *Oct3/4*) or the gross morphology of EBs formed during differentiation (Figures 3A and 3B). However, *Lphn2*-KD cells did not show complete cardiac differentiation in terms of cardiac gene expression and did not produce beating cells (Figures 3B and 3C, Videos S1 and S2).

To confirm the importance of LPHN2 in cardiac differentiation, we further established mouse *Lphn2*-knockout (KO) ESCs (Lee et al., 2019). IF analysis showed no LPHN2 expression in *Lphn2*-KO ESC-derived cells (Figure 3D). From day 10 to 14, wild-type ESC-derived cells began to contract (Video S3) and expressed α-SA with striations (Figure 3E). *Lphn2*-KO cells, however, did not generate contracting cardiac cells (Video S4).

As LPHN2 is a GPCR, we investigated its potential ligands. Two potential ligands have been reported for the LPHN family, particularly LPHN1 and LPHN3: α-latrotoxin (α-LTX) and fibronectin leucine-rich repeat transmembrane 3 (FLRT3), respectively (Langenhan et al., 2013; Lelianova et al., 1997; O'Sullivan et al., 2012). Cardiac differentiation was not significantly altered when cells were stimulated with α-LTX or FLRT3 (Figures 3F and 3G). Nonetheless, further research is required to determine the native

(C and D) qPCR analysis of (C) *Lphn2* and (D) *Pdpn* expression in the sorted cell populations on day 4 of differentiation. $^{**}p < 0.01$, $^{\#}$not significant, one-way ANOVA and *post hoc* Bonferroni test; $n = 3$ independent replicates. UD, undifferentiated.

(E and F) Differences in the mRNA expression of (E) *Mesp1* and (F) *Nkx2.5* in the sorted cell populations on day 4 of differentiation. Values are shown relative to day 0. $^{**}p < 0.01$, $^{\#}$not significant, one-way ANOVA and *post hoc* Bonferroni test; $n = 3$ independent replicates. UD, undifferentiated.

(G and H) Representative flow cytometric plots showing correlation in the expression of the cardiac progenitor cell markers PDPN, FLK-1, and PDGFR-α on day 4 of differentiation.

(I and J) Representative flow cytometric plots showing correlation between LPHN2 and PDPN expression on day 4 of differentiation.

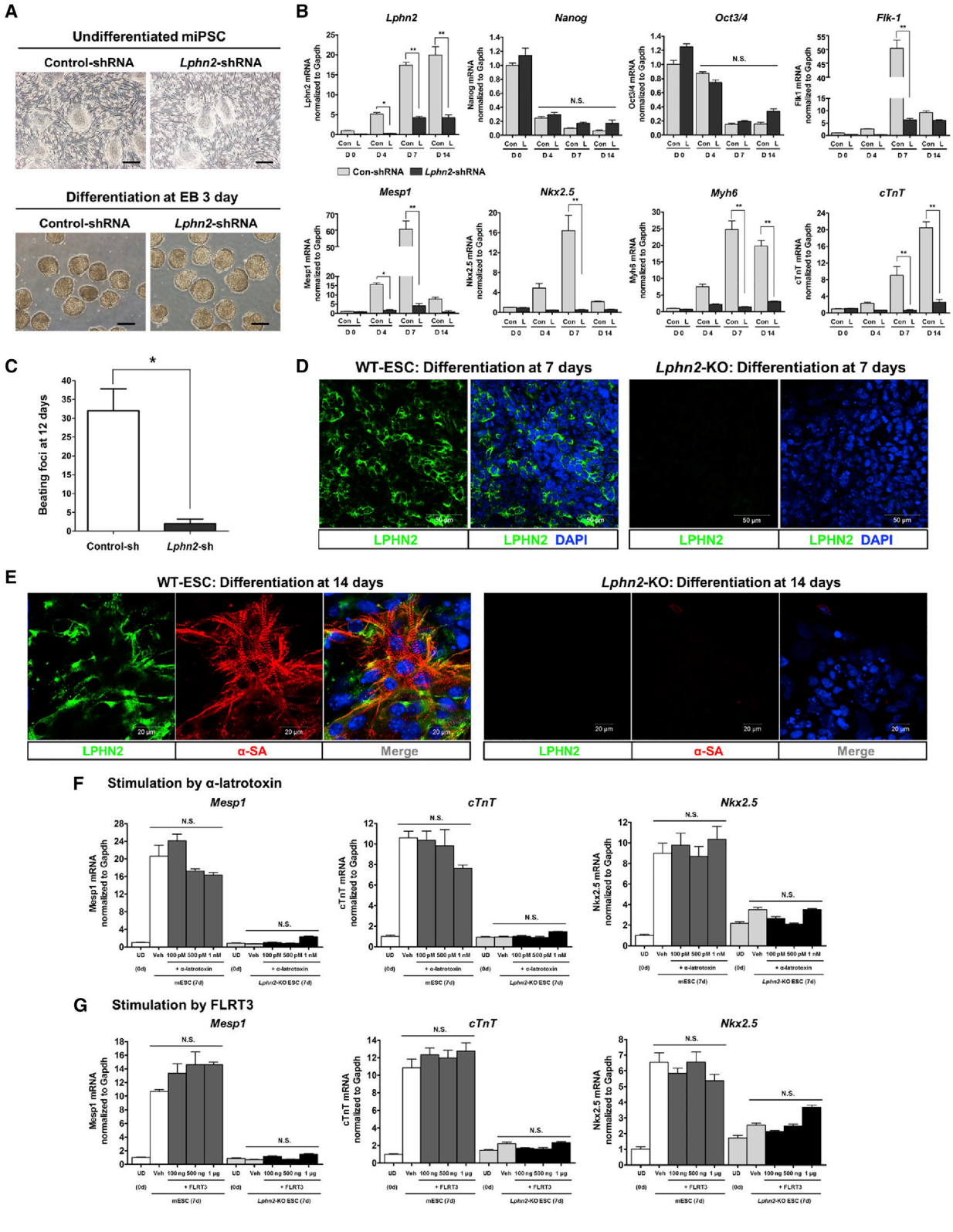

(legend on next page)

ligands involved in LPHN2-mediated cardiac differentiation and develop artificial agonists.

Mechanisms Underlying LPHN2-mediated Cardiac Differentiation

To investigate the molecular mechanisms underlying the induction of cardiac differentiation by LPHN2, we used the Phospho Explorer Antibody Array, which encompasses nearly all known signaling pathways. From the array data, we first calculated the degree of increased phosphorylation on differentiation day 4 relative to the phosphorylation on day 3 (phosphorylation ratio D4/D3) in three different groups: A, control-shRNA-transfected cells differentiating from mESCs; B, *Lphn2*-shRNA-transfected cells differentiating from mESCs; and C, *Lphn2*-KO cells differentiating from KO mESCs (Figure S5). Based on the phosphorylation ratios obtained, we delineated three different sets to construct a Venn diagram as follows. Set 1 included proteins with a phosphorylation ratio >1.5 for both groups A and B; set 2 included proteins with a >1.5-fold higher phosphorylation ratio for group A than for group B; and set 3 included proteins with a >1.5-fold higher phosphorylation ratio for group B than for group C (Figure 4A). The purpose of defining sets 1, 2, and 3 was to classify proteins according to a progressive increase in phosphorylation (from group C to A). The heatmap constructed from the data shown in the Venn diagram shows the differential phosphorylation ratios (Figure 4B). The proteins with specific phosphorylation sites in the intersecting region of the Venn diagram are shown in Figure 4C. LPHN2-dependent phosphorylation was the strongest for cyclin-dependent kinase 5 (CDK5) at Tyr15 (Figure 4C).

To confirm this finding, we performed western blot analysis with antibodies against phosphorylated CDK5 (Tyr15), as well as Src (Ser75) and P38MAPK (Tyr182), which are presumably downstream of CDK5. In wild-type mESCs, cardiac differentiation following exposure to cytokines significantly increased the phosphorylation of CDK5, Src, and P38MAPK on day 4 compared with that on day 3, whereas this phosphorylation was not observed in *Lphn2*-KO mESCs (Figures 5A and 5B). Treatment with roscovitine (a CDK5 inhibitor) or PP2 (a Src inhibitor) resulted in decreased phosphorylation of CDK5, Src, and P38MAPK. In contrast, upon application of SB 203580 (a P38MAPK inhibitor), neither CDK5 nor Src phosphorylation was inhibited; however, P38MAPK phosphorylation was decreased (Figures 5A and 5B). In *Lphn2*-KO mESCs, none of these inhibitors affected the level of phosphorylation, suggesting that LPHN2 signaling involved CDK5, Src, and P38MAPK activation.

qPCR analysis further confirmed that each inhibitor (roscovitine, PP2, and SB 203580) downregulated cardiac-specific gene expression (*Mesp1*, *Isl1*, *Tbx5*, and *cTnT*) in wild-type mESCs, but not in *Lphn2*-KO mESCs (Figure 5C). Therefore, our results suggested that CDK5 and Src interacted in parallel downstream of LPHN2 to induce cardiac differentiation, and P38MAPK, which is located downstream of CDK5 and Src, was also involved (Figure 5D). We concluded that LPHN2 was critical in the differentiation of PSCs into CPCs and CMCs, and CDK5, Src, and P38MAPK were key downstream molecules of LPHN2 signaling.

LPHN2 Expression in Human PSC Differentiation

Next, we analyzed the expression of LPHN2 (ADGRL2) in human PSCs. To differentiate human PSCs into CMCs efficiently, we optimized the previously developed protocols (Figure 6A). Similar to our findings in murine cells, *TNT* and *LPHN2* were not expressed in human dermal fibroblasts or undifferentiated human ESCs, including HUVECs (Figures 6B and S6A). As expected, *TNT* and *LPHN2* expression gradually increased throughout the process of

Figure 3. Functional Significance of LPHN2 during *In Vitro* Cardiac Differentiation

(A) Gross morphology of control induced pluripotent stem cells (iPSCs) and *Lphn2*-knockdown (KD) iPSCs transduced by control-shRNA and *Lphn2*-shRNA, respectively. No differences were observed in the colony formation or EB formation. Scale bar, 200 μm. EB, embryoid body.

(B) Effects of *Lphn2* KD on cardiac differentiation. Transcriptional profiling of *Lphn2*, *Nanog*, *Oct3/4*, *Flk-1*, *Mesp1*, *Nkx2.5*, *Myh6*, and *cTnT* in control iPSC- and *Lphn2*-KD iPSC-derived cells by qPCR. *$p < 0.05$, **$p < 0.01$, N.S., not significant, one-way ANOVA and *post hoc* Bonferroni test; $n = 3$ independent replicates.

(C) Quantification of spontaneous beating foci in control and *Lphn2*-KD cells on day 12 of cardiac differentiation. *$p < 0.05$, Mann-Whitney U test; $n = 4$ independent replicates.

(D) Immunostaining for LPHN2 (green) expression in wild-type embryonic stem cell (WT-ESC) and *Lphn2*-knockout (KO) ESC-derived cells on day 7 of cardiac differentiation. Blue, nuclear counterstaining with DAPI. Scale bar, 50 μm.

(E) WT-ESCs express LPHN2 (green) and α-SA (red) with striations at day 14 after differentiation, indicating cardiomyocyte differentiation, but *Lphn2*-KO ESCs did not differentiate into cardiomyocytes. Blue, nuclear counterstaining with DAPI. Scale bar, 20 μm.

(F and G) qPCR analysis of gene expression of cardiac-specific *Mesp1*, *Nkx2.5*, and *cTnT* after stimulation with presumptive ligands. Treatment with α-latrotoxin (F) and FLRT3 (G) did not increase the expression of cardiac lineage genes in mESCs or *Lphn2*-KO ESCs after 7 days under cardiac differentiation conditions. Values are shown relative to the expression in WT-mESCs on day 0. N.S., not significant, one-way ANOVA and *post hoc* Bonferroni test; $n = 3$ independent replicates. UD, undifferentiated; Veh, vehicle.

See also Videos S1, S2, S3, and S4.

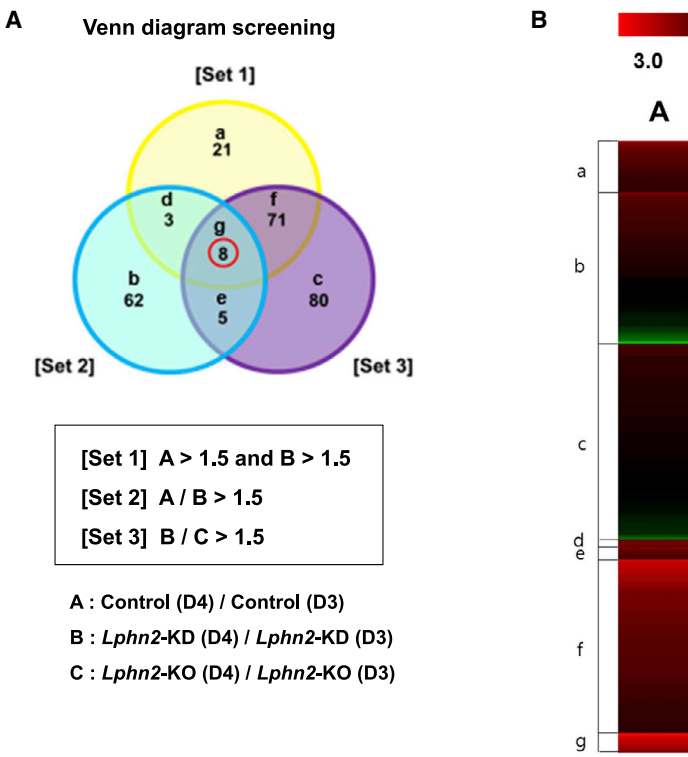

Figure 4. Screening of LPHN2-mediated Cardiac Differentiation Mechanisms Based on the Phospho Explorer Antibody Array

(A) A Venn diagram showing the intersection of sets 1, 2, and 3, with the most highly phosphorylated proteins in group A during differentiation of control-shRNA pluripotent stem cells. *Lphn2*-KO, *Lphn2*-knockout; *Lphn2*-KD, *Lphn2*-knockdown.

(B) Heatmap constructed from the data shown in (A) shows the differential phosphorylation ratios in groups A, B, and C.

(C) Phosphorylation sites of the most highly phosphorylated proteins in group A were considered as candidates for LPHN2 downstream signaling.

differentiation of human ESCs into CPCs and CMCs (Figure 6B). We examined the time course of LPHN2 expression during CMC differentiation using flow cytometry. LPHN2 expression gradually increased to 42.3%, and the cTNT expression level reached approximately 78.4% on day 14 (Figures 6C and 6D). Immunostaining analysis did not reveal the expression of LPHN2 in undifferentiated ESCs or HUVECs (Figures 6E and S6B). LPHN2, however, co-localized with KDR at day 7 of differentiation, and LPHN2$^+$ cells expressed NKX2.5 at day 14 (Figure 6E). Sequentially, IF staining confirmed that LPHN2 was expressed in beating CMCs expressing α-SA characterized by a striated morphology at day 28 post differentiation (Figure 6E).

When we sorted cells depending on the LPHN2 expression after 5 days of differentiation of human iPSCs toward CPCs, we observed significant enrichment of cardiac lineage cells in the LPHN2-positive cell population and could exclude cardiac lineage cells from the LPHN2-negative cell population (Figure 6F). Consistent with our findings in murine cells, human LPHN2$^+$ CPCs expressed other well-known CPC markers, such as SIRPα (Dubois et al., 2011), VCAM1 (Uosaki et al., 2011), and ROR1 (Halloin et al., 2019), in amounts higher than that expressed by LPHN2$^-$ cells. Under differentiation conditions, LPHN2$^+$ cells yielded SIRPα$^+$, VCAM1$^+$, and ROR1$^+$ CPCs with 90% efficiency, but LPHN2$^-$ cells failed to show CPC marker expression (10% efficiency) (Figure 6F).

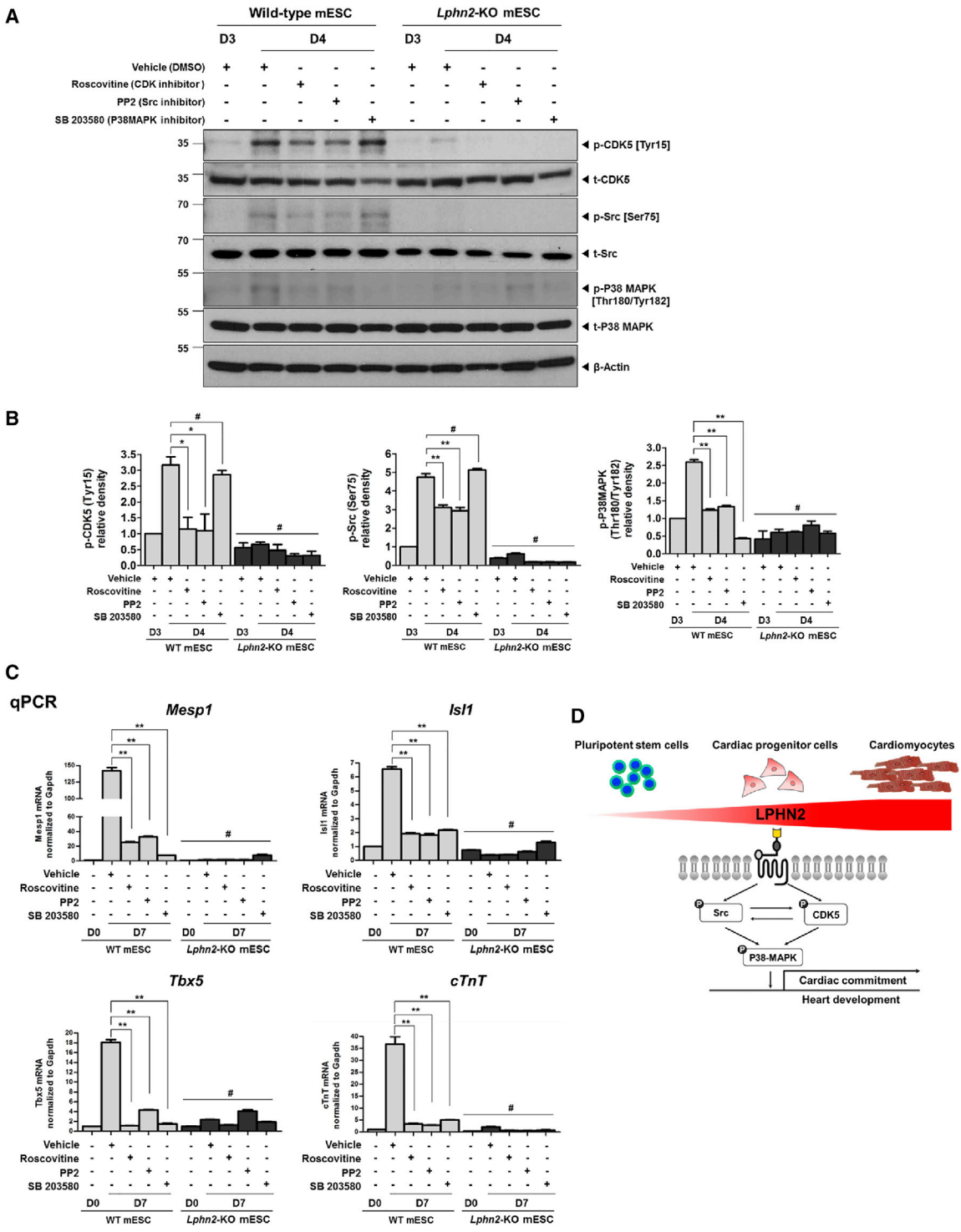

Figure 5. CDK5 Activated P38MAPK via Src and Induced Differentiation of Pluripotent Stem Cells into Cardiomyocytes

(A) Phosphorylation levels of CDK5, Src, and P38MAPK in wild-type mouse ESCs (mESCs) and *Lphn2*-knockout (KO) mESCs treated with the respective inhibitors during cardiac differentiation, as detected by western blotting.

(B) Quantification of the phosphorylation ratios of CDK5, Src, and P38MAPK in wild-type mESCs (WT mESCs) and *Lphn2*-KO mESCs. Values are shown relative to the phosphorylation ratio for the vehicle group of WT mESCs on day 3 of differentiation. $^{*}p < 0.05$, $^{**}p < 0.01$, $^{\#}$not significant, one-way ANOVA and *post hoc* Bonferroni test; $n = 3$ independent replicates.

(legend continued on next page)

To evaluate the multipotent potential, we purified KDR$^+$ or LPHN2$^+$ cells at day 5 by FACS analysis and re-cultured the purified cell populations for 14 days under EC or smooth muscle cell (SMC) differentiation conditions. Under the EC culture conditions, the KDR$^+$ and LPHN2$^+$ cell populations almost completely differentiated into CD31$^+$ or CD144$^+$ ECs with >90% efficiency (Figure 6G). In addition, the KDR$^+$ and LPHN2$^+$ cell populations predominantly differentiated into PDGFR-α^+ SMCs (Figure 6G). Immunostaining also showed that most LPHN2$^+$ cells at day 14 differentiated into VE-Cadherin$^+$ or CD31$^+$ ECs under differentiation conditions, similar to KDR$^+$ cells (Figures S6C and S6D).

Taken together, these data indicated that LPHN2 was highly expressed on the surface of human CPCs and CMCs. In conclusion, LPHN2 expression during human cardiac differentiation was identical to that in murine cardiac differentiation.

DISCUSSION

Although clinical trials have been performed for applying several types of stem cells in the treatment of acute myocardial infarction, CMCs derived from stem cells are not ready for clinical use. Extensive studies on pre-clinical and clinical cell therapies for heart diseases have employed several types of cells for cardiac repair. However, owing to the low efficiency of cardiac differentiation by various types of stem cells, effective methods to generate homogeneous cardiac cells in amounts sufficient for clinical applications are still lacking. Therefore, practical methods for generating homogeneous CMCs are a prerequisite for their eventual clinical application. Although CPCs have been identified using multiple markers (Chen and Wu, 2016), it is very challenging to isolate PSC-derived CPCs and CMCs *in vitro* because most cardiac-specific markers are intracellular molecules (Elliott et al., 2011) or transcription factors (Bu et al., 2009). Thus, cell-surface markers are required to purify CPCs and CMCs from heterogeneous cell populations during stem cell differentiation.

In this study, we demonstrated that a cardiac lineage-specific cell-surface marker, LPHN2, which is highly specific to CPCs and CMCs, possesses functional significance in mice and humans. Intriguingly, the mouse *Lphn2* gene is highly homologous to its human ortholog, with 95.8% identity. Recent studies have utilized SIRPα (Dubois et al., 2011), VCAM1 (Uosaki et al., 2011), ROR1 (Halloin et al., 2019), and PDPN (Birket et al., 2015) as cell-surface markers to purify human cardiac cell populations or enrich CMCs. However, SIRPα is not expressed in mouse cardiac cells, making it difficult to study its role and functional significance in KO or genetically modified models. In addition, cell sorting with anti-PDPN antibody was less useful in isolating mouse CPCs because of the differences in the PDPN protein homology between mice and humans. Herein, we reported several notable differences between LPHN2 and other CPC markers (Figures 7A and 7B).

The LPHN family includes three adhesion GPCRs (LPHN1–LPHN3) that mediate synaptic exocytosis caused by α-LTX in the venom of black widow spiders, which are an invertebrate species (Lelianova et al., 1997). However, their endogenous ligands and functions remain unclear (Ichtchenko et al., 1999). Similarly, there are three forms of LPHN present in vertebrates, each of which is expressed in different tissues. LPHN1 was first thought to be brain specific, but RNA blotting techniques revealed ubiquitous expression of the protein in all tissues at low levels (Boucard et al., 2014). In contrast, LPHN3 is expressed only in the brain. However, the potential mechanism underlying LPHN-mediated exocytosis remains unknown. As LPHN proteins are GPCRs, it might be expected that α-LTX triggers an intracellular G-protein-linked second-messenger cascade that ultimately leads to cardiac differentiation. Nevertheless, when we stimulated cells with α-LTX and another known LPHN3 ligand, FLRT3 (O'Sullivan et al., 2012), cardiac differentiation was not induced. These observations should therefore prompt further studies on GPCR-mediated signaling as well as innate and synthetic ligands for LPHN2-promoted cardiac differentiation.

We used the Phospho Explorer Antibody Array to investigate the molecular mechanism of LPHN2 in cardiac differentiation. The antibody array analysis showed that CDK5 phosphorylation at Tyr15 increased the most during cardiac differentiation from mESCs. Previous reports have shown that CDK5 is involved in myogenesis (Lazaro et al., 1997), whereas Src and P38MAPK are involved in ESC differentiation (Li et al., 2011) and heart function (Engel et al., 2006). In terms of a molecular hierarchy, Src is phosphorylated at S75 by CDK5 (Pan et al., 2011), and it has been shown to regulate P38MAPK activation. Thus, we first postulated that LPHN2 activated the downstream signaling cascade from CDK5 to Src and eventually to P38MAPK. LPHN2 activates P38MAPK via CDK5 and

(C) Gene expression analysis of *Mesp1*, *Isl1*, *Tbx5*, and *cTnT* in WT mESCs and *Lphn2*-KO mESCs treated with inhibitors of CDK5, Src, and P38MAPK on day 7 of cardiac differentiation. Values are shown relative to the expression in WT mESCs on day 0. $^{**}p < 0.01$, $^{\#}$not significant, one-way ANOVA and *post hoc* Bonferroni test; $n = 3$ independent replicates.

(D) Schematic illustration of the molecular mechanism of LPHN2-mediated cardiac differentiation via the CDK5-Src-P38MAPK signaling cascade.

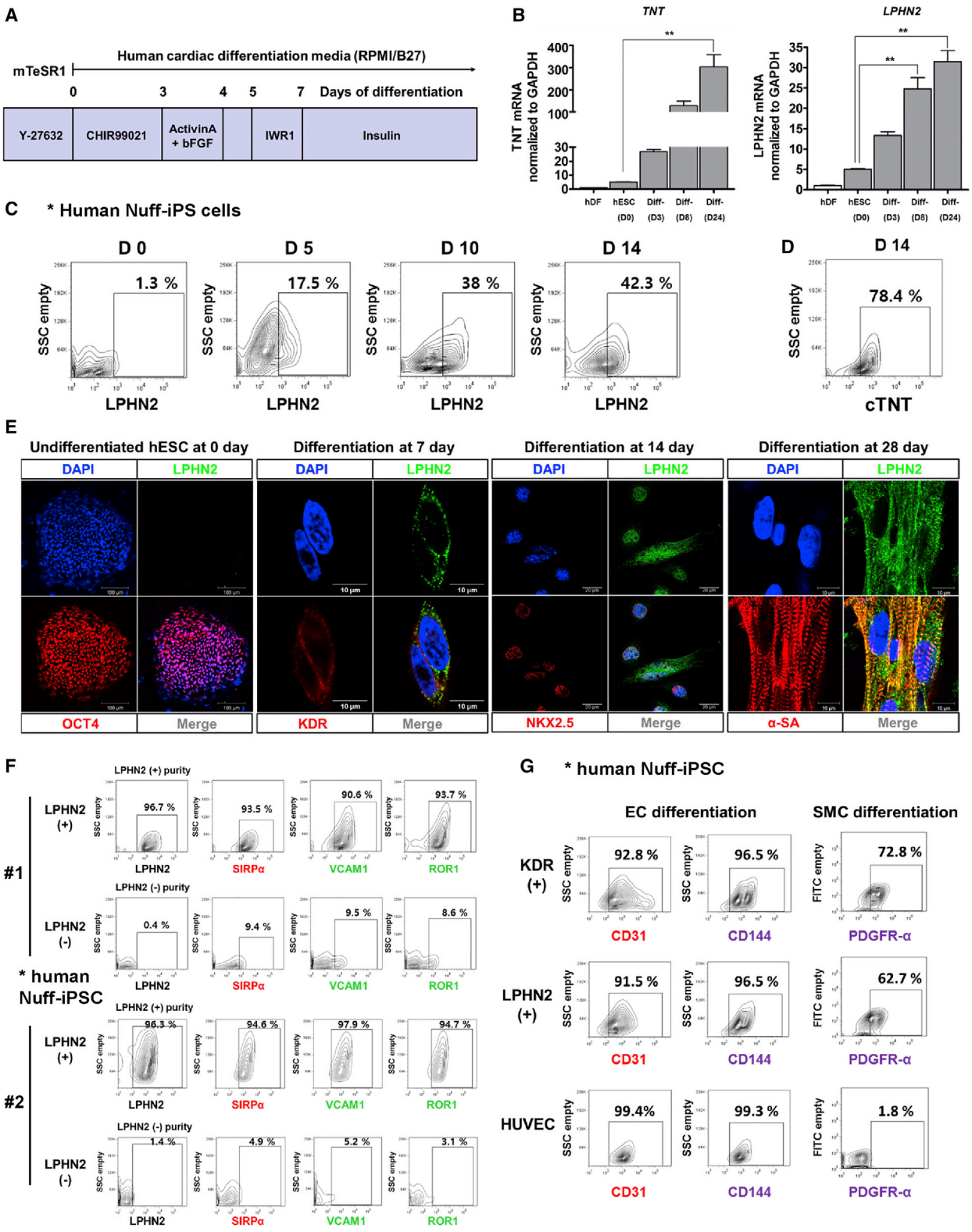

(legend on next page)

Src, which possibly affects the epithelial-mesenchymal transition events during differentiation to allow cardiac mesoderm formation (Graichen et al., 2008). However, our inhibitory experiments suggested that CDK5 and Src might act independently, rather than synergistically, during cardiac differentiation. In addition, it is interesting that CDK5, and not P38MAPK, appeared at the top of the molecular hierarchy, as Src and P38MAPK are better known for their functions in cardiac differentiation. CDK5 is known to be involved in myogenesis, but not in cardiac differentiation as such. Therefore, it is surprising that CDK5 phosphorylation was found to be critical for LPHN2 signaling during cardiac differentiation from PSCs.

In summary, we demonstrated that LPHN2 is a unique cell-surface marker of cardiac muscle progenitor cells and a functionally significant marker of cardiac differentiation. Analysis of the LPHN2 signaling pathway indicated that CDK5 is downstream of LPHN2 and interacts with Src kinase to induce P38MAPK phosphorylation, subsequently activating cardiac-specific gene transcription. The specific expression pattern of LPHN2 in PSC-derived cardiac lineage cells in mice and humans suggests that this receptor plays a pivotal and functional role across all strata of the cardiomyogenic lineage. Our findings, therefore, provide a strategy for achieving cardiac lineage cell differentiation that facilitates clinical application of stem cells in cardiovascular disease treatment.

EXPERIMENTAL PROCEDURES

Additional details on experimental procedures can be found in the Supplemental Experimental Procedures.

Ethics Statement

All experiments with human products were conducted with informed consent and were approved by the Institutional Review Board of Seoul National University Hospital (IRB no. H-0908-036-290).

Cell Lines and Maintenance

Cell culture was performed as previously described with slight modifications (Cho et al., 2010). C57BL/6-background mESCs (C57-mESCs; American Type Culture Collection [ATCC], cat. no. SCRC-1002) and iPSCs generated by FVB-background skin fibroblasts were cultured on a mitomycin C (Sigma-Aldrich)-treated STO (ATCC, cat. no. CRL-1503) or MEF (ATCC, cat. no. SCRC-1040) feeder layer in 0.1% gelatin (Sigma-Aldrich)-coated tissue culture dishes at 37°C in a 5% CO_2 atmosphere. All cell lines used in the study were regularly tested for mycoplasma, and no contamination was observed. The mESC culture medium was changed daily and composed of Dulbecco's modified Eagle's medium (DMEM; Gibco) with 2 mM L-glutamine, 10% fetal bovine serum (FBS; Gibco), 0.1 mM β-mercaptoethanol (Sigma-Aldrich, filter sterilized), 1% nonessential amino acids (Gibco), 50 IU/mL penicillin (Gibco), 50 mg/mL streptomycin (Gibco), and 2000 U/mL (20 ng/mL) recombinant leukemia inhibitory factor (LIF). The human ESC line ESI-049 was purchased from BioTime (cat. no. ES-702). Human ESCs were cultured with DMEM/F12 Glutamax (cat. no. 10565-018, Gibco) on an STO feeder layer. To generate human iPSCs from Nuff (newborn foreskin fibroblast) cells (cat. no. AMS.GSC-3006G, AMS Biotechnology), we introduced the reprogramming factors OCT4, SOX2, KLF4, and cMYC using lentiviruses (Takahashi et al., 2007). Human iPSCs were maintained on STO feeder cells with mTESR-1 medium (cat. no. 85851, STEMCELL Technologies).

EB Formation and Cardiac Differentiation

To assess the *in vitro* spontaneous differentiation potential, mESCs and iPSCs (Cho et al., 2010) were passaged in 0.1% gelatin-coated tissue culture dishes without feeder layers. Next, 1×10^6 cells were cultured by suspension in 100-mm Petri dishes containing EB medium (ESC medium without LIF). After 7 days, aggregated cells (EBs) were plated onto 0.1% gelatin-coated tissue culture dishes and cultured for another 7 or 14 days. Spontaneously contracting EBs were filmed with Olympus IX71 and Olympus DP71 digital cameras (15 fps/s at 680 × 512; Olympus). For cardiac differentiation of mouse PSCs, EBs were generated using AggreWell plates (STEMCELL Technologies) for 1 day and ultra-low attachment plates (Corning) for 3 days in the EB medium with activin A (10 ng/mL), BMP-4 (10 ng/mL), and bFGF (10 ng/mL). On day 4, EBs were attached to 0.1% gelatin-coated plates in the cardiac differentiation medium (35% Iscove's modified Dulbecco's medium, 65% DMEM/F12, 1% FBS, 2% B27, 2 mM L-glutamine, 0.1 mM 2-mercaptoethanol, and

Figure 6. LPHN2 Expression and Enriched CPC Potential in Human Pluripotent Stem Cells

(A) A schematic timeline demonstrating the major steps of the culturing procedure used for the directed differentiation of human pluripotent stem cells into cardiomyocytes.

(B) qPCR analysis of *TNT* and *LPHN2* expression in human embryonic stem cell (ESC)-derived cardiomyocytes. Expression values are shown relative to that in hDFs. **p < 0.01, one-way ANOVA and *post hoc* Bonferroni test; $n = 3$ independent replicates. hDF, human dermal fibroblast cell; hESC, human embryonic stem cell; Diff, differentiated.

(C) FACS plots for LPHN2 expression in undifferentiated human Nuff-iPS cells and during a time course of cardiac differentiation.

(D) FACS analysis of the cTNT expression in human Nuff-iPS cells during cardiac differentiation at day 14.

(E) Immunostaining for LPHN2 (green), OCT4 (red), KDR (red), NKX2.5 (red), and α-SA (red) expression in human ESCs and ESC-derived cardiomyocytes. Blue, nuclear counterstaining with DAPI.

(F) Flow cytometric analysis showing expression of CPC markers in sorted $LPHN2^+$ and $LPHN2^-$ populations at day 5 of differentiation.

(G) FACS measurements of CD31, CD144 after EC differentiation, and PDGFR-α after SMC differentiation of sorted populations.

A

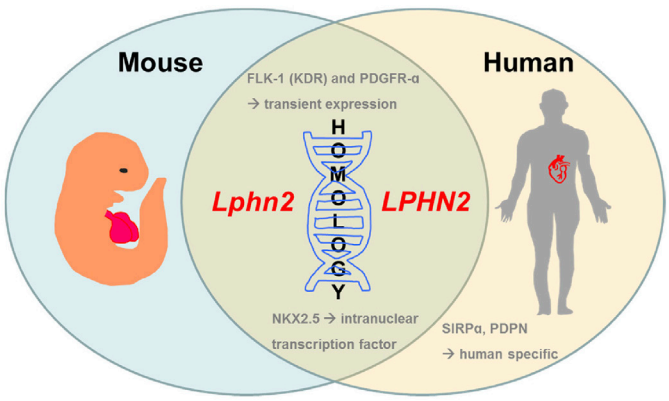

Figure 7. A Schematic Illustration and Summary Indicating the Applicability of LPHN2 as a Marker of Cardiac Differentiation

(A) Schematic illustration showing the differences in cardiac progenitor cell markers based on homology in mice and humans.

(B) Notable differences between LPHN2 and other reported cardiac progenitor cell markers for cardiac differentiation.

B

Markers of CPCs	LPHN2	NKX2.5 and PDPN	FLK-1 and PDGFR-α	SIRPα
Homology (Human and mouse)	Protein: 95.8 DNA: 87.4	1. NKX2.5 Protein: 89.3 DNA: 86.1 2. PDPN Protein: 48.1 DNA: 64	1. FLK-1 Protein: 86.7 DNA: 85.5 2. PDGFR-α Protein: 91.8 DNA: 86.5	Protein: 66.1 DNA: 74.4
Differences	1. Functional marker in mouse and human cardiomyogenic lineage cells 2. Easy to isolate requiring only one surface marker	1. No functional significance in mouse cardiac cells 2. Requiring two-color for FACS	1. Appear only transiently during development 2. Requiring two-color for FACS	1. Not expressed in mouse cardiac cells 2. Difficult to study the role and functional significance
Journal (Reference)	*Circulation* (Lee et al., 2019)	*Nat Biotechnol.* (Birket et al., 2015)	*Cell Stem Cell* (Kattman et al., 2011)	*Nat Biotechnol.* (Dubois et al., 2011)

antibiotics in the presence of 20 ng/mL EGF, 20 ng/mL bFGF, 40 ng/mL cardiotrophin-1, and 5 ng/mL VEGF). For cardiac differentiation of human ESCs and iPSCs, we optimized the previously described protocols (Lian et al., 2013). Briefly, human PSC colonies were detached by dispase (cat. no. 17105-041, Gibco) and dissociated into single cells and seeded in Matrigel (cat. no. 354277, Corning)-coated 35-mm dishes containing mTeSR1 medium (cat. no. 85851, STEMCELL Technologies) supplemented with 5 μM Y-27632 (cat. no. 72302, STEMCELL Technologies). When human PSCs reached 100% confluency, cardiac differentiation was induced in a monolayer supplemented with a mixture of cytokines that was changed sequentially. The cytokine treatments used were as follows: CHIR99021 (cat. no. 252917-06-9, Cayman) for 3 days, activin A (cat. no. 338-AC, R&D Systems) and bFGF (cat. no. 13256029, Invitrogen) for a day, and IWR1 (cat. no. I0161, Sigma-Aldrich) for 2 days. The medium was replaced once every 2 days with the human cardiac differentiation medium. The human cardiac differentiation medium was supplemented with B27 supplement in RPMI 1640 medium (cat. no. 11875-085, Gibco).

Statistics

All experiments were performed independently at least three times. For all cell types, multiple experiments were performed independently to verify the reproducibility of results. The number of samples (*n*) used for each experiment is indicated in the figures and their legends. The results are presented as the mean ± standard error of the mean (SEM). SPSS version 18.0 (SPSS) was used for all statistical analyses. Statistical analyses between two groups were conducted using the unpaired Student's t test or the Mann-Whitney U test, as appropriate. Comparison of more than two groups was performed using a one-way ANOVA, and *post hoc* comparisons were performed with the Bonferroni test. Statistical significance was defined at $p < 0.05$ and indicated as $^{*}p < 0.05$ and $^{**}p < 0.01$.

SUPPLEMENTAL INFORMATION

Supplemental information can be found online at https://doi.org/10.1016/j.stemcr.2021.03.003.

AUTHOR CONTRIBUTIONS

C.-S.L. designed and performed the majority of the experiments, conducted data analysis, prepared figures, and wrote the initial manuscript draft. H.-J.C. designed the experiments and contributed to manuscript writing. J.-W.L. assisted in conduction of the experiments. H.J.S. and J.C. assisted in performing the human PSC experiments. H.-S.K. designed the research, coordinated the research team, and finalized the manuscript.

DECLARATION OF INTERESTS

The authors declare no competing interests.

ACKNOWLEDGMENTS

This study was supported by grants from the Korea Health Technology Research and Development Project "Strategic Center of Cell and Bio Therapy" (grant HI17C2085) and "Korea Research-Driven Hospital" (grant HI14C1277) through the Korea Health Industry Development Institute, funded by the Ministry of Health and Welfare, Korea.

Received: September 22, 2020
Revised: March 1, 2021
Accepted: March 2, 2021
Published: April 1, 2021

REFERENCES

Anderson, G.R., Maxeiner, S., Sando, R., Tsetsenis, T., Malenka, R.C., and Sudhof, T.C. (2017). Postsynaptic adhesion GPCR latrophilin-2 mediates target recognition in entorhinal-hippocampal synapse assembly. J. Cell Biol. *216*, 3831–3846.

Birket, M.J., Ribeiro, M.C., Verkerk, A.O., Ward, D., Leitoguinho, A.R., den Hartogh, S.C., Orlova, V.V., Devalla, H.D., Schwach, V., Bellin, M., et al. (2015). Expansion and patterning of cardiovascular progenitors derived from human pluripotent stem cells. Nat. Biotechnol. *33*, 970–979.

Boucard, A.A., Maxeiner, S., and Sudhof, T.C. (2014). Latrophilins function as heterophilic cell-adhesion molecules by binding to teneurins: regulation by alternative splicing. J. Biol. Chem. *289*, 387–402.

Bu, L., Jiang, X., Martin-Puig, S., Caron, L., Zhu, S., Shao, Y., Roberts, D.J., Huang, P.L., Domian, I.J., and Chien, K.R. (2009). Human ISL1 heart progenitors generate diverse multipotent cardiovascular cell lineages. Nature *460*, 113–117.

Chen, I.Y., and Wu, J.C. (2016). Finding expandable induced cardiovascular progenitor cells. Circ. Res. *119*, 16–20.

Cho, H.J., Lee, C.S., Kwon, Y.W., Paek, J.S., Lee, S.H., Hur, J., Lee, E.J., Roh, T.Y., Chu, I.S., Leem, S.H., et al. (2010). Induction of pluripotent stem cells from adult somatic cells by protein-based reprogramming without genetic manipulation. Blood *116*, 386–395.

Dubois, N.C., Craft, A.M., Sharma, P., Elliott, D.A., Stanley, E.G., Elefanty, A.G., Gramolini, A., and Keller, G. (2011). SIRPA is a specific cell-surface marker for isolating cardiomyocytes derived from human pluripotent stem cells. Nat. Biotechnol. *29*, 1011–1018.

Elliott, D.A., Braam, S.R., Koutsis, K., Ng, E.S., Jenny, R., Lagerqvist, E.L., Biben, C., Hatzistavrou, T., Hirst, C.E., Yu, Q.C., et al. (2011). NKX2-5(eGFP/w) hESCs for isolation of human cardiac progenitors and cardiomyocytes. Nat. Methods *8*, 1037–1040.

Engel, F.B., Hsieh, P.C., Lee, R.T., and Keating, M.T. (2006). FGF1/p38 MAP kinase inhibitor therapy induces cardiomyocyte mitosis, reduces scarring, and rescues function after myocardial infarction. Proc. Natl. Acad. Sci. U S A *103*, 15546–15551.

Fox, I.J., Daley, G.Q., Goldman, S.A., Huard, J., Kamp, T.J., and Trucco, M. (2014). Stem cell therapy. Use of differentiated pluripotent stem cells as replacement therapy for treating disease. Science *345*, 1247391.

Graichen, R., Xu, X., Braam, S.R., Balakrishnan, T., Norfiza, S., Sieh, S., Soo, S.Y., Tham, S.C., Mummery, C., Colman, A., et al. (2008). Enhanced cardiomyogenesis of human embryonic stem cells by a small molecular inhibitor of p38 MAPK. Differentiation *76*, 357–370.

Greber, B., Wu, G., Bernemann, C., Joo, J.Y., Han, D.W., Ko, K., Tapia, N., Sabour, D., Sterneckert, J., Tesar, P., et al. (2010). Conserved and divergent roles of FGF signaling in mouse epiblast stem cells and human embryonic stem cells. Cell Stem Cell *6*, 215–226.

Halloin, C., Schwanke, K., Lobel, W., Franke, A., Szepes, M., Biswanath, S., Wunderlich, S., Merkert, S., Weber, N., Osten, F., et al. (2019). Continuous WNT control enables advanced hPSC cardiac processing and prognostic surface marker identification in chemically defined suspension culture. Stem Cell Rep. *13*, 775.

Hilger, D., Masureel, M., and Kobilka, B.K. (2018). Structure and dynamics of GPCR signaling complexes. Nat. Struct. Mol. Biol. *25*, 4–12.

Hudson, J., Titmarsh, D., Hidalgo, A., Wolvetang, E., and Cooper-White, J. (2012). Primitive cardiac cells from human embryonic stem cells. Stem Cells Dev. *21*, 1513–1523.

Ichtchenko, K., Bittner, M.A., Krasnoperov, V., Little, A.R., Chepurny, O., Holz, R.W., and Petrenko, A.G. (1999). A novel ubiquitously expressed alpha-latrotoxin receptor is a member of the CIRL family of G-protein-coupled receptors. J. Biol. Chem. *274*, 5491–5498.

Ieda, M., Fu, J.D., Delgado-Olguin, P., Vedantham, V., Hayashi, Y., Bruneau, B.G., and Srivastava, D. (2010). Direct reprogramming of fibroblasts into functional cardiomyocytes by defined factors. Cell *142*, 375–386.

Joo, H.J., Choi, D.K., Lim, J.S., Park, J.S., Lee, S.H., Song, S., Shin, J.H., Lim, D.S., Kim, I., Hwang, K.C., et al. (2012). ROCK suppression promotes differentiation and expansion of endothelial cells from embryonic stem cell-derived Flk1(+) mesodermal precursor cells. Blood *120*, 2733–2744.

Kattman, S.J., Witty, A.D., Gagliardi, M., Dubois, N.C., Niapour, M., Hotta, A., Ellis, J., and Keller, G. (2011). Stage-specific optimization of activin/nodal and BMP signaling promotes cardiac differentiation of mouse and human pluripotent stem cell lines. Cell Stem Cell *8*, 228–240.

Laflamme, M.A., Chen, K.Y., Naumova, A.V., Muskheli, V., Fugate, J.A., Dupras, S.K., Reinecke, H., Xu, C., Hassanipour, M., Police, S., et al. (2007). Cardiomyocytes derived from human embryonic

stem cells in pro-survival factors enhance function of infarcted rat hearts. Nat. Biotechnol. *25*, 1015–1024.

Langenhan, T., Aust, G., and Hamann, J. (2013). Sticky signaling–adhesion class G protein-coupled receptors take the stage. Sci. Signal. *6*, re3.

Lazaro, J.B., Kitzmann, M., Poul, M.A., Vandromme, M., Lamb, N.J., and Fernandez, A. (1997). Cyclin dependent kinase 5, cdk5, is a positive regulator of myogenesis in mouse C2 cells. J. Cell Sci. *110*, 1251–1260.

Lee, C.S., Cho, H.J., Lee, J.W., Lee, J., Kwon, Y.W., Son, T., Park, H., Kim, J., and Kim, H.S. (2019). Identification of latrophilin-2 as a novel cell-surface marker for the cardiomyogenic lineage and its functional significance in heart development. Circulation *139*, 2910–2912.

Lelianova, V.G., Davletov, B.A., Sterling, A., Rahman, M.A., Grishin, E.V., Totty, N.F., and Ushkaryov, Y.A. (1997). Alpha-latrotoxin receptor, latrophilin, is a novel member of the secretin family of G protein-coupled receptors. J. Biol. Chem. *272*, 21504–21508.

Li, X., Zhu, L., Yang, A., Lin, J., Tang, F., Jin, S., Wei, Z., Li, J., and Jin, Y. (2011). Calcineurin-NFAT signaling critically regulates early lineage specification in mouse embryonic stem cells and embryos. Cell Stem Cell *8*, 46–58.

Lian, X., Zhang, J., Azarin, S.M., Zhu, K., Hazeltine, L.B., Bao, X., Hsiao, C., Kamp, T.J., and Palecek, S.P. (2013). Directed cardiomyocyte differentiation from human pluripotent stem cells by modulating Wnt/beta-catenin signaling under fully defined conditions. Nat. Protoc. *8*, 162–175.

O'Sullivan, M.L., de Wit, J., Savas, J.N., Comoletti, D., Otto-Hitt, S., Yates, J.R., 3rd, and Ghosh, A. (2012). FLRT proteins are endogenous latrophilin ligands and regulate excitatory synapse development. Neuron *73*, 903–910.

Oikonomopoulos, A., Kitani, T., and Wu, J.C. (2018). Pluripotent stem cell-derived cardiomyocytes as a platform for cell therapy applications: progress and hurdles for clinical translation. Mol. Ther. *26*, 1624–1634.

Pan, Q., Qiao, F., Gao, C., Norman, B., Optican, L., and Zelenka, P.S. (2011). Cdk5 targets active Src for ubiquitin-dependent degradation by phosphorylating Src(S75). Cell. Mol. Life Sci. *68*, 3425–3436.

Takahashi, K., Tanabe, K., Ohnuki, M., Narita, M., Ichisaka, T., Tomoda, K., and Yamanaka, S. (2007). Induction of pluripotent stem cells from adult human fibroblasts by defined factors. Cell *131*, 861–872.

Uosaki, H., Fukushima, H., Takeuchi, A., Matsuoka, S., Nakatsuji, N., Yamanaka, S., and Yamashita, J.K. (2011). Efficient and scalable purification of cardiomyocytes from human embryonic and induced pluripotent stem cells by VCAM1 surface expression. PLoS One *6*, e23657.

Yang, L., Soonpaa, M.H., Adler, E.D., Roepke, T.K., Kattman, S.J., Kennedy, M., Henckaerts, E., Bonham, K., Abbott, G.W., Linden, R.M., et al. (2008). Human cardiovascular progenitor cells develop from a KDR+ embryonic-stem-cell-derived population. Nature *453*, 524–528.

Yu, P., Pan, G., Yu, J., and Thomson, J.A. (2011). FGF2 sustains NANOG and switches the outcome of BMP4-induced human embryonic stem cell differentiation. Cell Stem Cell *8*, 326–334.

Stem Cell Reports, Volume *16*

Supplemental Information

Adhesion GPCR Latrophilin-2 Specifies Cardiac Lineage Commitment through CDK5, Src, and P38MAPK

Choon-Soo Lee, Hyun-Jai Cho, Jin-Woo Lee, HyunJu Son, Jinho Chai, and Hyo-Soo Kim

Supplemental Information

Adhesion GPCR, latrophilin-2, specifies cardiac lineage commitment through CDK5, Src, and P38MAPK

Choon-Soo Lee,[1,2,5] Hyun-Jai Cho,[4,5] Jin-Woo Lee,[1,2] HyunJu Son,[1,2] Jinho Chai,[1,3] and Hyo-Soo Kim,[1,2,3*]

[1]Strategic Center of Cell & Bio Therapy, Seoul 03080, Republic of Korea

[2]Molecular Medicine and Biopharmaceutical Sciences, Graduate School of Convergence Science and Technology, Seoul National University, Seoul, Republic of Korea

[3]Program in Stem Cell Biology, Seoul National University College of Medicine, Seoul, Republic of Korea

[4]Department of Internal Medicine, Seoul National University Hospital, Seoul, Republic of Korea

Figure S1

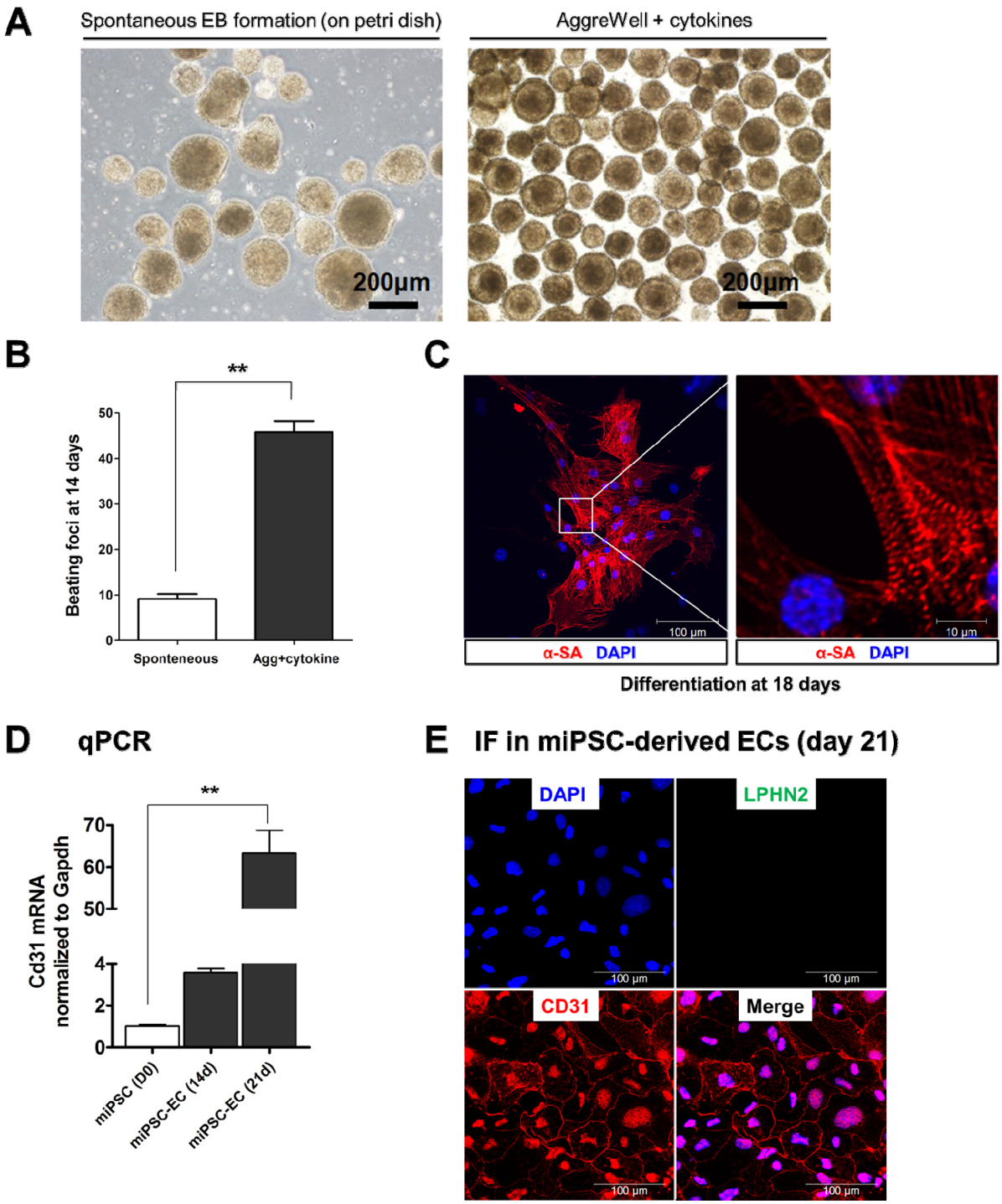

Figure S1 (Related to Figure 1). Optimized culture conditions for cardiac differentiation and LPHN2 expression in mouse iPSC-derived ECs.

(**A**) Comparison of the size and shape of EBs using Petri dishes and AggreWell plates at day 4 after differentiation. The EB populations on AggreWell plates are uniform in size and shape relative to those of the petri dish culture. Scale bar, 200 μm. **(B)** Beating foci count in cardiac differentiation culture at 14 days. $^{**}P < 0.01$, Mann–Whitney U test, $n = 8$ independent biological replicates. **(C)** Immunostaining for α-sarcomeric actinin (α-SA, red) in cardiac differentiation culture at day 18. Blue, nuclear counterstain with 4, 6-diamidino-2-phenylindole (DAPI). A white rectangle in the left image indicates the regions shown at higher magnification. Scale bars, 100 μm (left panels) or 10 μm (right panels). **(D)** Gene expression analysis of mouse iPSC-derived endothelial cells analyzed by qPCR for *Cd31*. Expression values are shown relative to that of miPSCs (D0). $^{**}P < 0.01$, ANOVA test and *post hoc* Bonferroni test, $n = 3$ independent replicates. **(E)** Immunostaining for LPHN2 (green) and CD31 (red) in mouse iPSC-derived ECs. Scale bar, 100 μm. Scale bar, 100 μm.

Figure S2

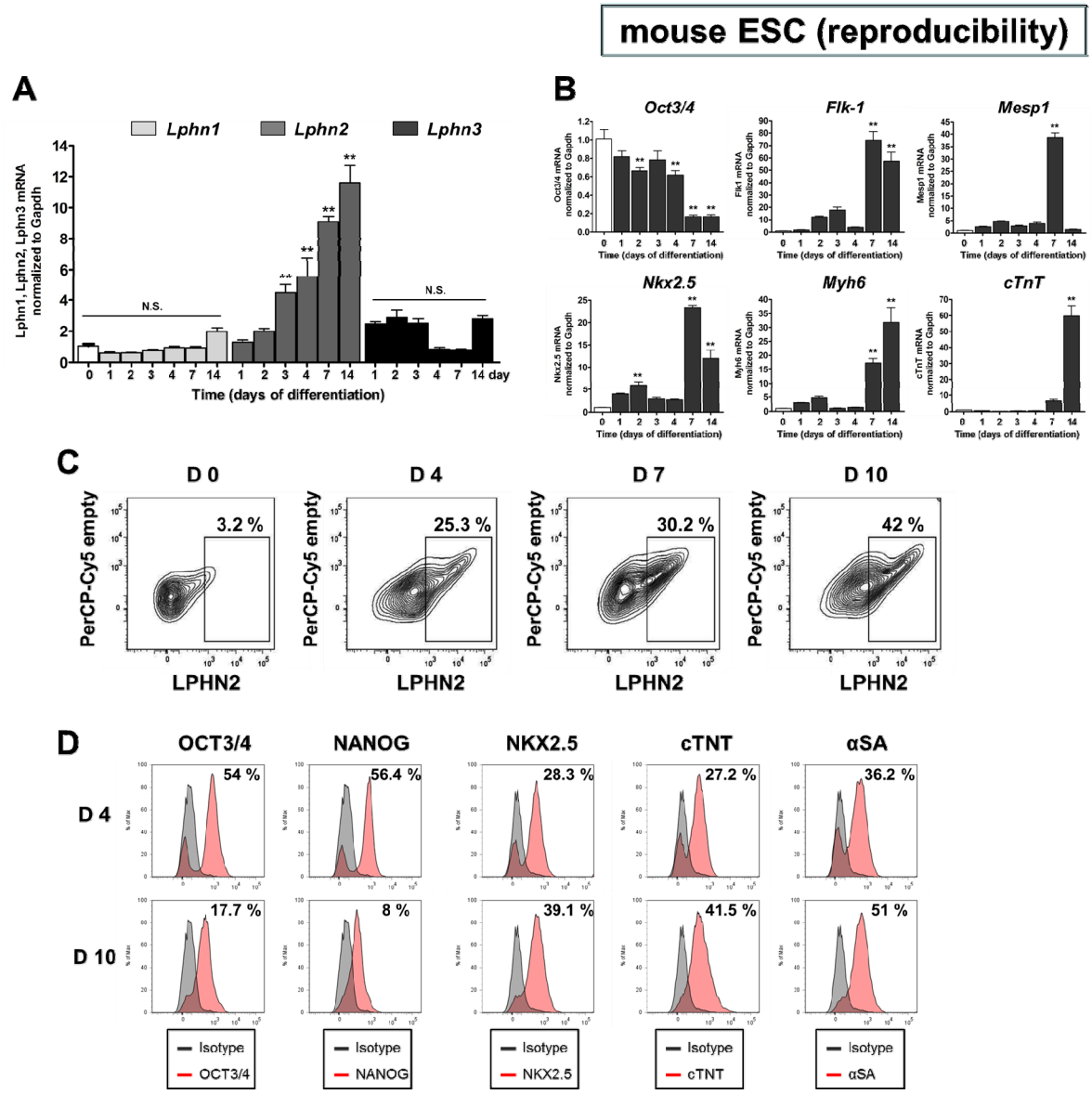

Figure S2 (Related to Figure 1). Reproducibility of iPSC findings in mouse ESCs.
(A) Gene expression analysis by qPCR of *Lphn1*, *Lphn2,* and *Lphn3* in ESCs following cardiac differentiation. Values are shown relative to day 0. $^{**}P < 0.01$, N.S. (not significant), ANOVA test and *post hoc* Bonferroni test, $n = 3$ independent replicates. **(B)** mRNA expression levels of *Oct3/4*, *Flk-1*, *Mesp1*, *Nkx2.5*, *Myh6,* and *cTnT* in ESC-derived cells during cardiac differentiation. $^{**}P < 0.01$, ANOVA test and *post hoc* Bonferroni test, $n = 3$ independent replicates. **(C)** Sequential changes in LPHN2 expression in ESC-derived cardiac lineage populations by FACS analysis. **(D)** FACS analysis of multiple markers (OCT3/4, NANOG, NKX2.5, cTNT, and αSA) in ESC-derived cells during cardiac differentiation.

Figure S3

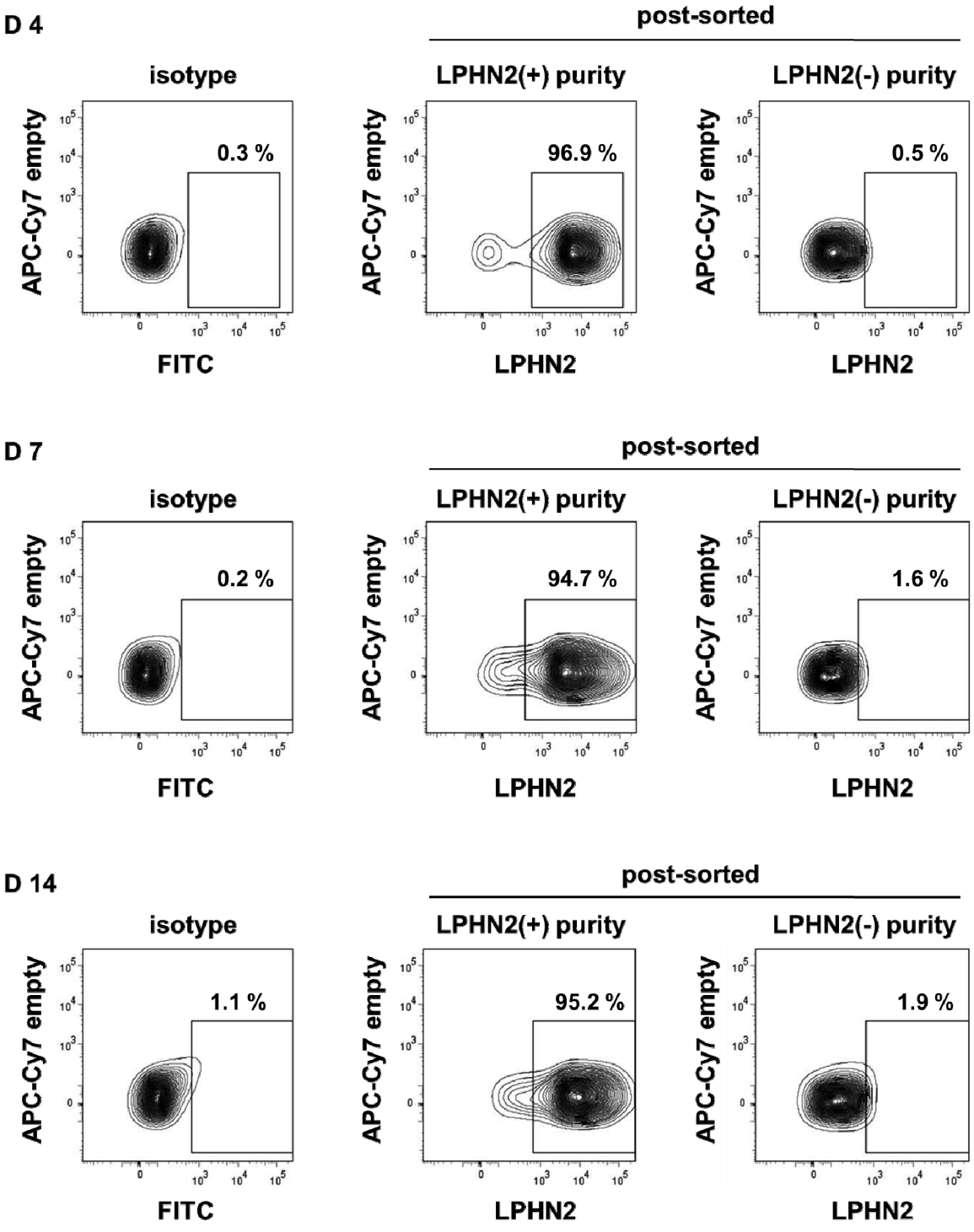

Figure S3 (Related to Figure 2). Sorting purity of LPHN2^{+} and LPHN2^{-} fractions in iPSC-derived cells during cardiac differentiation.

Figure S4

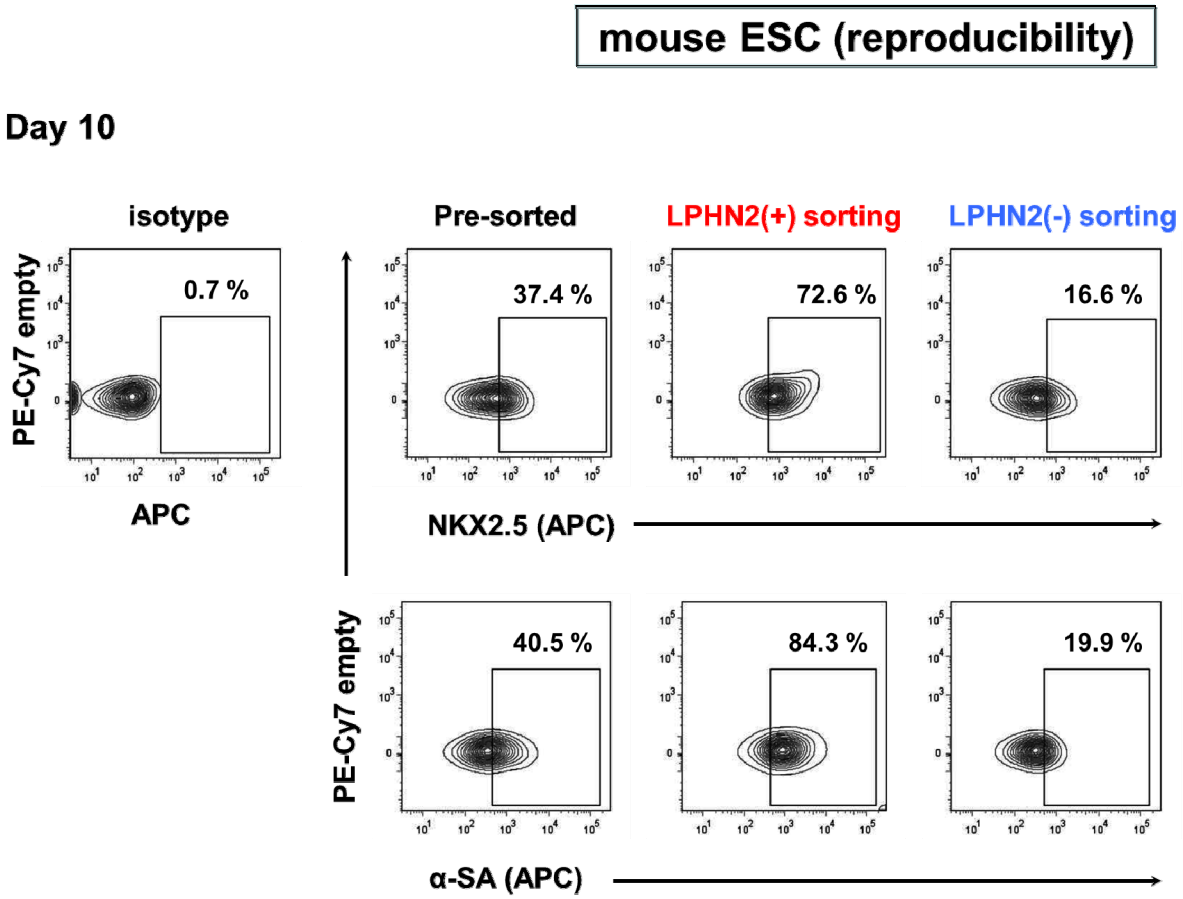

Figure S4 (Related to Figure 2). Enriched expression of NKX2.5 and α-SA sorted by LPHN2 in mouse ESCs.

Representative FACS plot showing surface expression of NKX2.5 and α-SA at 10 days after cardiac differentiation for pre-sort, $LPHN2^{+}$, and $LPHN2^{-}$ fraction in mouse ESC-derived cells.

Figure S5

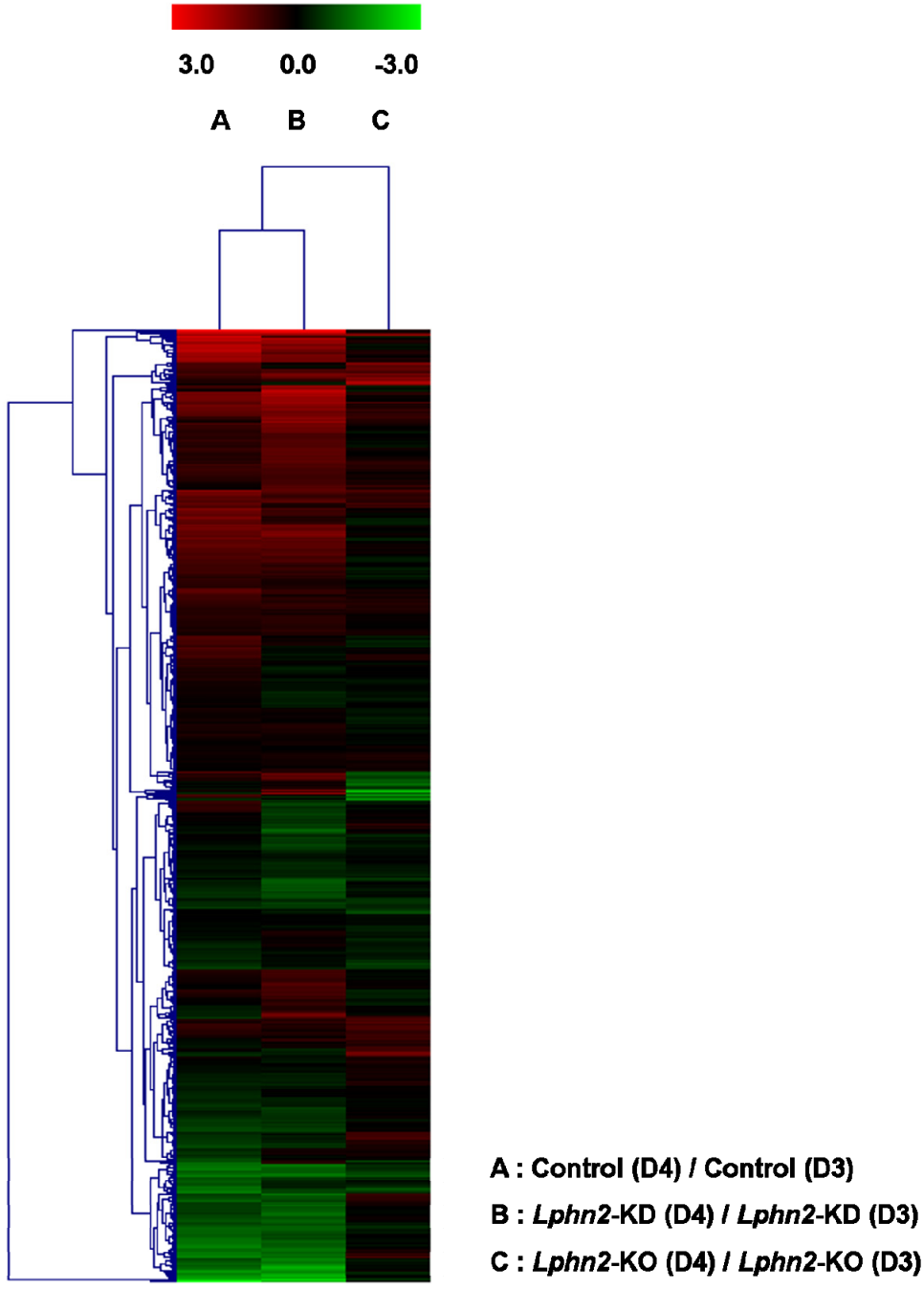

Figure S5 (Related to Figure 4). Heat map based on a Phospho Explorer Antibody Array. Differential phosphorylation ratio between groups A (control (D4)/control (D3)), B (*Lphn2*-KD (D4)/*Lphn2*-KD (D3)), and C (*Lphn2*-KO (D4)/*Lphn2*-KO (D3)).

Figure S6

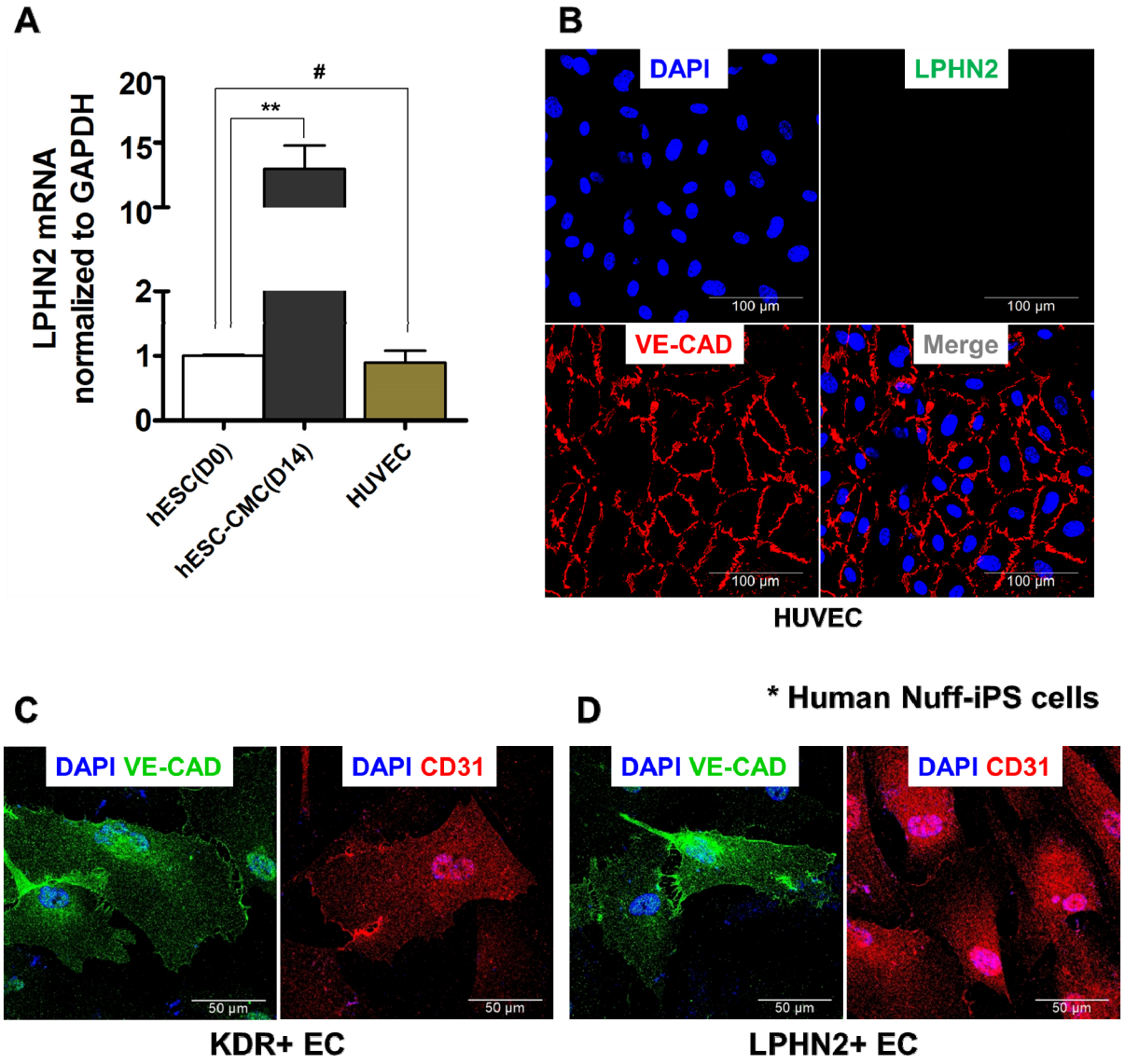

Figure S6 (Related to Figure 6). LPHN2 expression in HUVEC and endothelial differentiation potential of the KDR-positive or LPHN2-positive population.

(A) qPCR analysis of *LPHN2* expression in human ESCs, human ESC-derived CMCs and HUVECs. Expression values are shown relative to that of hESCs (D0). $^{**}P < 0.01$, #*P* = N.S. (not significant), ANOVA test and *post hoc* Bonferroni test, $n = 3$ independent replicates. **(B)** Immunostaining for LPHN2 (green) and VE-Cadherin (red) in HUVECs. Blue, nuclear counterstaining with 4, 6-diamidino-2-phenylindole (DAPI). Scale bar, 100 µm.

(C) Immunofluorescence analysis for EC markers (VE-Cadherin and CD31) in KDR^+ cells differentiated toward endothelial lineages on day 14. Blue, nuclear counterstaining with 4, 6-diamidino-2-phenylindole (DAPI). **(D)** Immunostaining of VE-Cadherin and CD31 in $LPHN2^+$ cells on day 14 of endothelial differentiation. Blue, nuclear counterstaining with 4, 6-diamidino-2-phenylindole (DAPI). Scale bar, 50 μm.

Supplemental Movie Legends

Movie S1 (Related to Figure 3). Beating foci following control-iPSCs and cardiac differentiation. On day 10 of cardiac differentiation, control-shRNA transduced iPSCs exhibited robust beating.

Movie S2 (Related to Figure 3). Beating foci following *Lphn2* knockdown (KD) and cardiac differentiation. On day 10 of cardiac differentiation, *Lphn2*-shRNA transduced iPSCs did not beat spontaneously.

Movie S3 (Related to Figure 3). Beating foci following wild-type ESCs and cardiac differentiation. On day 10 of cardiac differentiation, there were several spontaneous beating foci in wild-type ESCs.

Movie S4 (Related to Figure 3). Beating foci following *Lphn2* knockout (KO) and cardiac differentiation. On day 10 of cardiac differentiation, there were not spontaneous beating foci in *Lphn2*-KO ESCs.

Table S1. PCR primers used in this study

Primer	Sequence	Access Number
Mouse Lphn1	Forward 5′- AAGACATGAATGCCACCGAA -3′ Reverse 5′- CTCTTGGGGGAACACCAACT -3′	NM_181039.2
Mouse Lphn2	Forward 5′- GCTGCAAGCTGGTTGACACT -3′ Reverse 5′- GATGCAGATAGCCAGGCAGA -3’	NM_001081298.1
Mouse Lphn3	Forward 5′- TTTATAGGACCGGCGACCTT -3′ Reverse 5′- TACATGAGTCCAAAGGCCCA -3′	NM_198702.2
Mouse Nanog	Forward 5′- CAGAAAAACCAGTGGTTGAAGACTAG -3′ Reverse 5′- GCAATGGATGCTGGGATACTC -3	NM_001289828.1
Mouse Oct3/4	Forward 5′- GAGGATCACTTGGGGTACA -3′ Reverse 5′- CTCGAAGCGACAGATGGTG -3′	NM_013633.3
Mouse Flk-1	Forward 5′- GGCGGTGGTGACAGTATCTT -3′ Reverse 5′- CTCGGTGATGTACACGATGC -3′	NM_010612.2
Mouse PdgfR-α	Forward 5’- TCCATGCTAGACTCAGAAGTCA -3’ Reverse 5’- TCCCGGTGGACACAATTTTTC -3’	NM_001083316.2
Mouse Mesp1	Forward 5’- TGTACGCAGAAACAGCATCC -3’ Reverse 5’- TTGTCCCCTCCACTCTTCAG -3’	NM_008588.2
Mouse Nkx2.5	Forward 5’- GACAAAGCCGAGACGGATGG -3’ Reverse 5’- CTGTCGCTTGCACTTGTAGC -3’	NM_008700.2
Mouse Myh6	Forward 5’- ACGGTGACCATAAAGGAGGA -3’ Reverse 5’- TGTCCTCGATCTTGTCGAAC -3’	NM_001164171.1
Mouse cTnT (Tnnt2)	Forward 5′- CAGAGGAGGCCAACGTAGAAG -3′ Reverse 5′- CTCCATCGGGGATCTTGGGT -3’	NM_001130174.2
Mouse Tbx5	Forward 5′- GGAGCCTGATTCCAAAGACA -3′ Reverse 5′- TTCAGCCACAGTTCACGTTC -3′	NM_011537.3
Mouse Isl1	Forward 5′- CACTATTTGCCACCTAGCCAC -3′ Reverse 5′- AAATACTGATTACACTCCGCAC -3′	NM_021459.4
Mouse Cd31 (Pecam1)	Forward 5′- TGCAGGAGTCCTTCTCCACT -3′ Reverse 5′- ACGGTTTGATTCCACTTTGC -3’	NM_001032378.2
Mouse Gapdh	Forward 5′- GACCCCTTCATTGACCTCAAC -3′ Reverse 5′- CTTCTCCATGGTGGTGAAGA -3′	NM_001289726.1
Human LPHN2	Forward 5′- CTGGTTGCAGAATGCGAAGT -3′ Reverse 5′- CAAATCTTGTCATCCGTCCG -3	NM_001297704.1
Human GAPDH	Forward 5′- AACATCATCCCTGCCTCTAC -3′ Reverse 5′- CCCTGTTGCTGTAGCCAAAT -3′	NM_001256799.2

Table S2. Antibodies, Cytokines, and Reagents

Primary antibody	**Cat. #**	**Company**	**Application**
Anti-Mouse CD309 (FLK-1) Biotin	13-5821-82	eBioscience	FC
Anti-Mouse CD140a (PDGFR-α) APC	17-1401-81	eBioscience	FC
Anti-Human/Mouse OCT3/4 PE	12-5841-80	eBioscience	FC
Nanog	3580	cell signaling	FC
Oct3/4	sc-9081	Santa Cruz	IF
Nkx2.5	sc-8697	Santa Cruz	FC
Anti-Cardiac Troponin T	ab10214	Abcam	FC
Anti-Sarcomeric Alpha Actinin	ab9465	Abcam	FC, IF
Monoclonal Anti-α-Sarcomeric Actin	A2172	Sigma-Aldrich	IF
GFAP	sc-6170	Santa Cruz	FC
AFP	sc-15375	Santa Cruz	FC
PECAM-1 (CD31)	sc-1506-R	Santa Cruz	IF
VE-Cadherin	sc-6458	Santa Cruz	IF
Latrophilin-2	sc-47091	Santa Cruz	FC
Anti-LPHN2	ab101833	Abcam	IF
Phospho-CDK5 [Tyr15]	sc-12918	Santa Cruz	WB
Phospho-Src [Ser75]	Ab194520	Abcam	WB
Phospho-P38MAPK [Thr180/Tyr182]	9211	cell signaling	WB
CDK5	684502	BioLegend	WB
Src	2109	cell signaling	WB
P38MAPK	9212	cell signaling	WB
β-actin	sc-1615	Santa Cruz	WB
Anti-VEGF Receptor 2 (FLK-1)	ab10972	Abcam	IF
Lectin from Ulex europaeus (UEA-I)	L9006	Sigma-Aldrich	IF
Anti-human CD172a/b (SIRPα/β)	323804	BioLegend	FC
Human VCAM-1/CD106	FAB5649G	R&D systems	FC
Human ROR1	FAB2000G	R&D systems	FC
Human CD31	555446	BD Pharmingen	FC
Human CD144	17-1449-42	eBioscience	FC
Human PDGFR-α	FAB1264A	R&D systems	FC

Secondary Antibody	**Cat. #**	**Company**	**Application**
Streptavidin PE	12-4317-87	eBioscience	FC
Alexa Fluor 488 Donkey Anti-Goat IgG	A11055	Invitrogen	IF, FC
Alexa Fluor 488 Donkey anti-Rabbit IgG	A21206	Invitrogen	IF
Alexa Fluor 488 Goat Anti-Chicken IgG	A11039	Invitrogen	IF
Alexa Fluor 555 Goat Anti-Mouse IgG	A21422	Invitrogen	IF
Alexa Fluor 555 Donkey anti-Rabbit IgG	A31572	Invitrogen	IF
Alexa Fluor 555 Donkey Anti-Goat IgG	A21432	Invitrogen	IF
Alexa Fluor 555 Goat anti-Mouse IgM(μ chain)	A21426	Invitrogen	IF
Streptavidin, Alexa Fluor 555 Conjugate	S32355	Invitrogen	IF
Alexa Fluor 647 Donkey anti-Rabbit IgG	A31573	Invitrogen	IF, FC
Alexa Fluor 647 Donkey anti-Goat IgG	A21447	Invitrogen	IF, FC
Alexa Fluor 647 Donkey anti-Mouse IgG	A31571	Invitrogen	IF, FC
Alexa Fluor 647 Goat anti-Mouse IgM(μ chain)	A21238	Invitrogen	IF
Cytokines and Reagents	**Cat. #**	**Company**	
Activin A	338-AC	R&D Systems	
BMP-4	5020-BP	R&D Systems	
bFGF	13256029	Invitrogen	
EGF	236-EG	R&D Systems	
Cardiotrophin-1	612-CD	R&D Systems	
VEGF 164	493-MV	R&D Systems	
Recombinant human VEGF 165	293-VE-050	R&D Systems	
Recombinant human PDGF-BB	220-BB-010	R&D Systems	
Leukaemia Inhibitory Factor (LIF)	ESG1107	Millipore	
α-Latrotoxin	LSP-130	Alomone labs	
FLRT3	2795-FL	R&D Systems	

FC : Flow Cytometry, IF : ImmunoFluorescence, WB : Western Blot

Supplemental Experimental Procedures

RNA isolation and qPCR

Total RNA was prepared using QIAshredder and RNeasy Mini Kit (Qiagen, Inc.) according to the manufacturer's instructions. RNA (1 μg) was converted into cDNA using the ReverTra Ace® qPCR RT Master Mix (TOYOBO). qPCR was performed using FastStart Universal SYBR Green Master (Roche) with specific primers. Primer sequences are provided in Table S1. qPCR samples were run on an ABI PRISM-7500 sequence detection system (Applied Biosystems). Data are presented as relative quantification values. Gapdh was run simultaneously as a control and used for normalization.

Antibody array

1) Sample preparation: The protein was extracted by using protein extraction buffer (Fullmoon biosystems, Sunnyvale, CA) containing 1% protease inhibitor cocktail (Sigma, St. Louis, Mo) and 1% phosphotase inhibitor cocktail (Sigma, St. Louis, Mo) and lysis beads (Fullmoon biosystems, Sunnyvale, CA). After extraction, the protein solution was purified using gel matrix column that was included in antibody array assay kit (Fullmoon biosystems, Sunnyvale, CA). The column was vortex-mixed at 5 seconds and hydration-treated at 60 minutes on room temperature. After hydration, the column was centrifuged at 750 g for 2 minutes. After centrifuge, the column was placed into a collect tube and the 100 μl of protein sample was transferred into column. The column was centrifuged at 750 g for 2 minutes. The concentration of purified sample was measured with BCA protein assay kit (Pierce, Rockford, Ill) using NanoPhotometerTM (Implen, UK). Moreover, the purity of purified sample was confirmed on UV spectrum.

2) Phospho Explorer Antibody Array: The 50 μg of protein sample was filled up 75 μl with labeling buffer and treated 3 μl of the 10 μg/μl biotin/DMF solution. The sample was incubated at room temperature for 90 min with mixing. After incubation, the sample was treated 35 μl of stop reagent and incubated at room temperature for 30 min with mixing. The antibody microarray slide (Fullmoon biosystems, Sunnyvale, CA) was treated 30 ml of blocking solution in a petri dish and incubated on shaker at 60 rpm for 30 min at room temperature and washed with distilled water. This step was replicated three times. After blocking, the slide was rinsed with Milli-Q grade water. The labeled sample was mixed in 6 ml of coupling solution. The blocked array slide was incubated with coupling mixture on shaker at 60 rpm for 2 hours at room temperature into coupling dish. After coupling, the slide was washed 6 times with 30 ml of washing solution into petri dish on shaker at 60 rpm for 5 minutes. Next, the slide rinsed with Milli-Q grade. The 30 μl of 0.5 mg/ml Cy3-streptavidin (GE Healthcare, Chalfont St. Giles, UK) was mixed in 30 ml of detection buffer. The coupled array slide was treated with detection mixture into petri dish on shaker at 60 rpm for 20 minutes at room temperature. After detecting, the slide was washed 6 times with 30 ml of washing solution into petri dish on shaker at 60 rpm for 5 minutes. Next, the slide rinsed with Milli-Q grade water.

3) Data acquisition and analysis: The slide scanning was performed using GenePix 4100A scanner (Axon Instrument, USA). The slides were absolutely dried before the scanning and scanned within 24~48 hours. The slides were scanned at 10 μm resolution, optimal laser power and PMT. After got the scan image, they were grided and quantified with GenePix 7.0 Software (Axon Instrument, USA). The normalization data were analyzed using Genowiz 4.0TM (Ocimum Biosolutions, India). This normalization makes the average intensity of all samples numerically equivalent to the average intensity of the all genes. Moreover, the *p*-value (one-

sample *t*-test) was calculated using MeV 4.9.0 Software (TM4 Development Group, USA). After analyzing, the data about protein information was annotated using UniProt DB. The phosphorylation ratio was calculated using the following formula (phosphorylated and matching unphosphorylated values are denoted by phospho and unphospho in both the differentiation day 3 and day 4).

Phosphorylation ratio = (phospho of differentiation day 4/unphospho of day 4) / (phospho of differentiation day 3/ unphospho of day 3)

Antibody array results are accessible at the GEO database (accession number, GSE92923).

Western blot

Cells were harvested and lysed for 30 minutes in lysis buffer containing protease inhibitors (Roche, Basel, Switzerland). Total protein (40 μg) was immunoblotted with primary antibodies against phospho-CDK5 [Tyr15] (Santa Cruz Biotechnology, Dallas, TX, USA; goat polyclonal; molecular weight = 35 kDa), phospho-Src [Ser75] (Abcam, Cambridge, UK; rabbit polyclonal; molecular weight = 60 kDa), phospho-P38MAPK [Thr180/Tyr182] (Cell Signaling, Danvers, MA, USA; rabbit polyclonal; molecular weight = 43 kDa), total-CDK5 (BioLegend, San Diego, USA; mouse monoclonal; molecular weight = 35 kDa), total-Src (Cell Signaling, Danvers, MA, USA; rabbit monoclonal; molecular weight = 60 kDa), total-P38MAPK (Cell Signaling, Danvers, MA, USA; rabbit polyclonal; molecular weight = 43 kDa), and β-actin (Santa Cruz Biotechnology, Dallas, TX, USA; goat polyclonal; molecular weight = 43 kDa). Horseradish peroxidase (HRP)-conjugated anti-rabbit IgG (for phospho-Src, and phospho-P38MAPK, total-Src, total-P38MAPK; Santa Cruz Biotechnology, Dallas, TX, USA), anti-goat IgG (for phospho-CDK5 and β-actin; Santa Cruz Biotechnology, Dallas, TX, USA) and anti-mouse IgG (for total-

CDK5; Santa Cruz Biotechnology, Dallas, TX, USA) antibodies were used as secondary antibodies. Amersham ECL western blotting detection reagents (GE Healthcare Life Sciences, Chicago, IL, USA) were used for detection. Quantification of band intensity was analyzed using TINA software, version 2.0 (RayTest, Straubenhardt, Germany), and was normalized to the total-form antibody.

Endothelial and smooth muscle differentiation of Human PSC

For endothelial and smooth muscle differentiation of human PSCs, we optimized using the previously described protocols. Human PSCs were directed towards the cardiac progenitor cells until day 5. After day 5 sorting, KDR^+ or $LPHN2^+$ cells were induced in EGM-2MV medium (Cat. #: CC-3124, LONZA) supplemented with 50 ng/ml VEGF and 5 μM SB431542 for endothelial, or 8 ng/ml PDGF-BB and 10 ng/ml bFGF for smooth muscle differentiation.

Immunofluorescence staining

Cells were fixed with 2% paraformaldehyde (PFA, Wako) for 10 minutes at room temperature. After being washed with PBS and blocked with PBS containing 0.05% Triton-X100 and 1% BSA, the cells were incubated with primary antibodies for 18 hrs at 4°C. After washing, corresponding secondary antibodies were applied for 1 h at room temperature. The nuclei were counterstained with 4', 6-diamidino-2-phenylindole (DAPI) and mounted using the fluorescent mounting medium (DAKO). Fluorescent images were acquired with an LSM710 confocal microscope (Zeiss) and a confocal microscope Leica TCS SP8 (Leica Microsystems, Wetzlar, Germany). Information of the primary and secondary antibodies for immunofluorescence is provided in Table S2.

Flow cytometric analysis and cell sorting

EBs were harvested and treated with Accutase (eBioscience) for 5 min at 37°C to dissociate cells. Cells were then washed with PBS, stained with specific antibodies (Table S2) for lineage markers. The fixation and permeabilization buffer kit (R&D system) was used as recommended in the manufacturer's instructions for intracellular staining of OCT3/4, NANOG, cTNT, α-SA, NKX2.5, GFAP, and AFP. Analysis of stained cells and sorting were performed by flow cytometry using fluorescence-activated cell sorting (FACS) Canto II TM or Aria II TM (BD Biosciences) and obtained data were analyzed by FlowJo (Tree Star, Ashland, OR, USA).

Lentiviral transduction

For *Lphn2* knockdown in iPSCs, five shRNA constructs targeting different regions of the *Lphn2* gene were used (Sigma-Aldrich, SHCLNV, MISSION® shRNA Lentiviral Transduction Particles, TRCN0000238691, TRCN0000238692, TRCN0000238693, TRCN0000238694, TRCN0000238695). Non-Target shRNA Control Transduction Particles (Sigma-Aldrich, SHC216V) was used as the shRNA negative control. Transduction was performed according to manufacturer's instructions. At 48 hrs after transduction, protein-iPSCs were selected in growth medium containing puromycin (5 μg/ml, Sigma-Aldrich). Transduced iPSCs were analyzed for *Lphn2* knockdown efficiency using qPCR.

Lphn2-KO ESCs

Lphn2-KO ESCs ($Lphn2^{tm1a\ (EUCOMM)\ Hmgu}$, EUCOMM) were purchased from EUCOMM. *Lphn2*-KO ESCs were cultured in knockout DMEM (Gibco) including 10% fetal bovine serum,

0.1 mM β-mercaptoethanol (Sigma-Aldrich, filter sterilized), 2 mM L-glutamine, 50 IU/mL penicillin, 50 mg/mL streptomycin (Gibco), and LIF (2000 U/mL) on MEF as feeder-layer cells.